

# Effective field theory methods to model compact binaries

**Stefano Foffa<sup>1</sup> and Riccardo Sturani<sup>2</sup>**

(1) Département de Physique Théorique, Université de Genève, CH-1211 Geneva, Switzerland

(2) ICTP South American Institute for Fundamental Research  
Instituto de Física Teórica, Universidade Estadual Paulista, Sao Paulo, SP  
011040-070, Brasil

E-mail: [stefano.foffa@unige.ch](mailto:stefano.foffa@unige.ch), [sturani@ift.unesp.br](mailto:sturani@ift.unesp.br)

**Abstract.** In this short review we present a self-contained exposition of the effective field theory method approach to model the dynamics of gravitationally bound compact binary systems within the post-Newtonian approximation to General Relativity. Applications of this approach to the conservative sector, as well as to the radiation emission by the binary system are discussed in their salient features. Most important results are discussed in a pedagogical way, as in-depths and details can be found in the referenced papers.

PACS numbers: 04.20.-q,04.25.Nx,04.30.Db

## 1. Introduction

The existence of gravitational waves (GW) is an unavoidable prediction of General Relativity (GR) and astrophysical objects bound in binary systems are prototypical, even though not exclusive, sources of GWs. The precise evidence of a system emitting GWs comes from the celebrated ‘‘Hulse-Taylor’’ binary pulsar [1], whose orbital decay rate is in agreement with the GR prediction to about one part in a thousand [2], see also [3, 4, 5, 6] for more examples of observed GW emission from pulsar binary systems.

A network of earth-based, kilometer-sized GW observatories is currently under development with the goal of detecting GWs: the two Laser Interferometer Gravitational-Wave Observatories (LIGO) in the US and the French-Italian Virgo interferometer in Italy have been taking data at unprecedented sensitivities for several years, see e.g. [7] for recent results, and are now undergoing upgrades to their advanced stage, see e.g. [8] for a recent review (another smaller detector belonging to the network is the German-British Gravitational Wave Detector GEO600). The gravitational detector network is planned to be joined by the Japanese detector KAGRA by the end of this decade [9] and by an additional interferometer in India by the beginning of the next decade. The advanced detector era is planned to start in the year 2015 and it is expected that few years will be necessary to reach planned sensitivity, which should allow several detections of GW events per year [10].

Compact binary systems offer a privileged setting where to confront GR with observations, and their dynamics has been the object of intensive studies since the advent of GR. Here we focus on the *post-Newtonian* (PN) approximation to GR, see e.g. [11] for a review, which consists in a perturbative expansion around Minkowski space. The expansion parameter is the relative velocity  $v$  of the binary constituents ‡, or equivalently the gravitational field strength  $G_N M/r$  (where  $G_N$  is the standard Newton constant,  $M$  the total mass of the binary system, and  $r$  the orbital separation between its constituents), as by the virial theorem  $v^2 \sim G_N M/r$ .

The approach to solving for the dynamics of the two body problem adopted here relies on the non-relativistic formulation of GR originally proposed in [12], see also [13] for a review, which sets the problem in an Effective Field Theory (EFT) framework.

The use of field theory tools like Feynman diagrams in GR is not a novelty, see e.g. [14, 15, 16] for pioneer work in this direction. With respect to these early works, the EFT approach has the merit of recognizing scale separation as an organizational principle for systematic computation at the Lagrangian level.

Indeed the two body problem exhibits a clear separation of scales: the size of the compact objects  $r_s$ , like black holes and/or neutron stars, the orbital separation  $r$  and the gravitational wave-length  $\lambda$ . Using again the virial theorem the hierarchy  $r_s < r \sim r_s/v^2 < \lambda \sim r/v$  can be established. The EFT approach allows to use the scale separation of the physical problem to arrange a transparent and systematic power counting in the expansion parameter, with physics at different scales related by

‡ We posit the speed of light  $c = 1$ .

*renormalization group flow*. It has many common features with ordinary quantum field theory (Feynman diagrams, divergence regularizations, logarithmic running of physical observables) as both the *classical* effective field theory described here and *quantum* field theory share properties belonging to any *field theory*.

The interest in the analytical description of gravitationally bound binary systems has been revived in recent times by the activity of the above mentioned GW observatories whose output is particularly sensitive to the GW phase. It is very important to have an accurate description of the waveform, whose shape depends on the source motion, for both maximizing the detection probability and for extracting the highest possible physical content from candidate events. Moreover data analysis techniques involve the generation of several tens of thousands to millions waveforms, thus requiring their analytical knowledge in order to have quick and efficient data analysis pipelines.

In particular the dynamical quantities allowing to determine physical observables like the phase of the GW signal, are the energy of the bound orbit and the emitted flux of GWs. Since signals falling in the detector band sensitivity are in the very last stage of the coalescence, the binary system orbits are expected to have circularized by then [17, 18], so the analytical quantities to be computed are the energy of circular orbits and the gravitational flux as a function of the relative velocity of the binary constituents.

Moreover recent progress have made available numerical-relativity waveforms emitted in the last  $O(10)$  orbits of a binary system (including merger and ring-down) [19]. In order to construct complete *hybrid* waveforms encompassing all the stages of a coalescence from inspiral to merger and ring-down, the highest possible accuracy on the analytical inspiral phase is necessary to reduce the length of the numerically evolved part of the waveform, which is in general very time consuming [20].

It is then expected that GW observations and numerical modeling will bring new inputs from both the phenomenological and the theoretical numerical side to the two body problem in General Relativity, whereas the effective field theory approach described here is giving new momentum to the analytical studies on the theoretical side.

## 2. General Theory

The effective field theory approach to the GR two-body problem is analog to other effective field theory approaches adopted to study specific systems in particle physics, like the heavy quark field theory [21, 22]. We want to study the dynamics of a pair of heavy and compact objects (black holes/neutron stars) interacting through the exchange of gravitational degrees of freedom and emitting GWs.

The effective Lagrangian  $\mathcal{S}_{ext}$  of *any* extended object of size  $r_{source}$  interacting with a gravitational field with characteristic length-scale variation  $L \gg r_{source}$ , can be

parametrized in terms of its mass  $m$ , spin tensor  $S_{ab}$  and higher order multipoles [23] §

$$\mathcal{S}_{ext} \supset \int d\tau \left( -m - \frac{1}{2} S_{ab} \omega_\mu^{ab} u^\mu + c_Q I_{ij} E^{ij} + c_J J_{ij} B^{ij} + c_O I_{ijk} \partial_i E_{jk} + \dots \right), \quad (1)$$

where  $\omega_\mu^{ab}$  is the spin connection coupling to the total angular momentum, while the electric (magnetic) tensor  $E_{ij}$  ( $B_{ij}$ ) is defined by

$$\begin{aligned} E_{ij} &= C_{\mu\nu ij} u^\mu u^\nu, \\ B_{ij} &= \epsilon_{i\mu\nu\rho} u^\rho C^{\mu\nu}_{j\sigma} u^\sigma, \end{aligned} \quad (2)$$

decomposing the Weyl tensor  $C_{\mu\alpha\nu\beta}$  analogously to the electric and magnetic decomposition of the standard electromagnetic tensor  $F_{\mu\nu}$ . This amounts to decompose the source motion in terms of the world-line of its center of mass and moments describing its internal dynamics. The  $I_{ij}$ ,  $I_{ijk}$ ,  $J_{ij}$  tensors are the lowest order in an infinite series of source moments, the 2<sup>n</sup>-th electric (magnetic) moment in the above action scale at leading order as  $m r_{source}^n$  ( $m v r_{source}^n$ ), and they couple to the Taylor expanded  $E_{ij}$  ( $B_{ij}$ ) which scales as  $L^{-(1+n)}$ , showing that the above multipole expansion is an expansion in terms of  $r_{source}/L$ .

Note that the multipoles, beside being intrinsic, can also be induced by the tidal gravitational field or by the intrinsic angular momentum (spin) of the source. For quadrupole moments, the intrinsic case will be explicitly dealt with in subsec. 3.2, whereas the tidal induced quadrupole moments  $I_{ij}, J_{ij}|_{tidal} \propto E_{ij}, B_{ij}$  give rise to the following terms in the effective action

$$\mathcal{S}_{tidal} = \int d\tau \left[ c_E E_{ij} E^{ij} + c_B B_{ij} B^{ij} \right]. \quad (3)$$

This is also in full analogy with electromagnetism, where for instance particles with no permanent electric dipole experience a quadratic coupling to an external electric field. Eq. (3) can be used to describe a single, spin-less compact object in the field of its binary system companion. Considering that the Riemann tensor generated at a distance  $r$  by a source of mass  $m$  goes as  $m/r^3$ , the finite size effect given by the  $E_{ij} E^{ij}$  term goes as  $c_E m^2/r^6$ . For dimensional reasons  $c_E \sim G_N r_{source}^5$  [12], thus showing that the finite size effects of a spherical symmetric body in the binary potential are  $O(Gm/r)^5$  times the Newtonian potential, a well known result which goes under the name of *effacement principle* [24] (the coefficient  $c_E$  actually vanishes for black holes in 3 + 1 dimensions [25, 26]).

One may consider the inclusion in  $\mathcal{S}_{ext}$  of monopole terms linear in curvature invariants like  $c_R \int d\tau R$  and  $c_V \int R_{\mu\nu} \dot{x}^\mu \dot{x}^\nu$ . However these terms can be safely omitted as they vanish by the Einstein equations outside the source generating them||. As linear terms in the Ricci tensor and Ricci scalar cannot appear, the terms involving the least number of derivatives are the ones written above in eq. (1), in terms of the (traceless part of the) Riemann tensor.

§ We adopt the  $(-, +, +, +)$  signature,  $\tau$  is the proper time running along the source world-line,

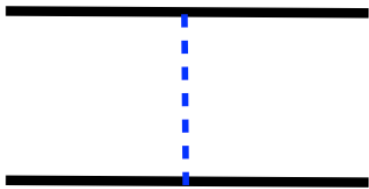


**Figure 1.** Feynman graph accounting for the Newtonian potential.



**Figure 2.** Corrections to the Newtonian potential due to gravity non-linearities. The left (right) diagram starts contributing at the 1(2)PN order.

We will focus in the next section onto the derivation of the effective potential of a binary system, obtaining the general relativistic realization of the Newtonian potential. This is obtained by *integrating out* the degrees of freedom that mediate the gravitational attraction to obtain a Fokker-type action  $\mathcal{S}_{eff}$  describing the instantaneous interaction between objects parametrized by world-lines  $x_{A,B}$ . Formally this is achieved by computing the Feynman path integral

$$e^{i\mathcal{S}_{eff}} = \int \mathcal{D}h_{\mu\nu} e^{i[S_{bulk}(\eta_{\mu\nu}+h_{\mu\nu})+S_{ext}(x_a, \eta_{\mu\nu}+h_{\mu\nu})]}, \quad (4)$$

where  $S_{bulk}$  involves only the gravitational degrees of freedom and is given by the standard Einstein Hilbert action plus the harmonic gauge fixing term corresponding to the harmonic gauge used in [11]

$$S_{bulk} = S_{EH} + S_{GF}, \quad S_{GF} \equiv -\Lambda^2 \int dt d^d x \sqrt{-g} \Gamma^\mu \Gamma_\mu, \quad \Gamma^\mu \equiv \Gamma_{\alpha\beta}^\mu g^{\alpha\beta}, \quad (5)$$

with  $\Lambda = (32\pi G_N)^{-1/2}$  in  $d = 3$ .

Because of the non-linearities of the Einstein Hilbert action and of the gravity-matter coupling, the functional integral in eq. (4) cannot be performed exactly, but only perturbatively. For instance the leading perturbative order is represented by the diagram in fig. 1: it accounts for the potential generated by the exchange of a gravitational degree of freedom. Performing the above functional integral is equivalent to solving the non-linear equations iteratively around the linear solution at the level of the action: the perturbative solution can then be organized in Feynman diagrams as it is customary done in quantum field theory, however we stress once again that no quantum effects will be considered here.

$u^\mu \equiv dx^\mu/d\tau$  is the 4-velocity of the center of mass.

|| Such terms give  $\delta$ -like, unobservable contributions to the classical potential. Equivalently, it can be shown that the field redefinition  $g_{\mu\nu} \rightarrow g_{\mu\nu} + \delta g_{\mu\nu}$  with

$$\delta g_{\mu\nu} = \int d\tau \frac{\delta(x^\alpha - x^\alpha(\tau))}{\sqrt{-g}} \left[ \left( -c_R + \frac{c_V}{2} \right) g_{\mu\nu} - c_V u_\nu u_\nu \right]$$

can be used to set to zero the above terms linear in the curvature, see [13] for details.

In order to show in practice how the iterative solutions can be used to efficiently generate the dynamics of the problem, we find convenient to decompose the metric in the form

$$g_{\mu\nu} = e^{2\phi/\Lambda} \begin{pmatrix} -1 & A_j/\Lambda \\ A_i/\Lambda & e^{-c_d\phi/\Lambda}\gamma_{ij} - A_iA_j/\Lambda^2 \end{pmatrix}, \quad (6)$$

with  $\gamma_{ij} = \delta_{ij} + \sigma_{ij}/\Lambda$ ,  $c_d = 2\frac{(d-1)}{(d-2)}$ , according to the metric ansatz proposed in [27, 28] and reminiscent of the one first used in [29]. On the previous ansatz  $\mathcal{S}_{bulk}$  reduces to

$$\mathcal{S}_{bulk} \simeq \int dt d^d x \left( -c_d(\partial\phi)^2 + \dots \right), \quad (7)$$

where only the kinetic term of the gravitational field  $\phi$  has been explicitly written. The  $\phi$  coupling to the source, which is implicit from eq. (1), is  $m/\Lambda \int d\tau \phi (1 + \mathcal{O}(v^2))$  and neglecting all interaction terms of the field  $\phi$ , the Gaussian integration over  $\phi$  in eq. (4) can be done exactly and leads to

$$S_{eff} = -m_1 \int d\tau_1 - m_2 \int d\tau_2 + i \frac{m_1 m_2}{2c_d \Lambda^2} \int d\tau_1 d\tau_2 G(\tau_1 - \tau_2, x_1(\tau_1) - x_2(\tau_2)), \quad (8)$$

where  $G(t, x)$  is the Feynman Green function

$$G(t, x) = -i \int \frac{dk_0}{2\pi} \int_{\mathbf{k}} e^{-ik_0 t + i\mathbf{k}\cdot x} \frac{1}{\mathbf{k}^2 - k_0^2 - i\epsilon}, \quad (9)$$

with  $\int_{\mathbf{k}} \equiv \int \frac{d^d k}{(2\pi)^d}$ . It is now crucial to take the non-relativistic limit in order to work at a given order in  $v$ . This is achieved by observing that the wave-number  $k^\mu \equiv (k^0, \mathbf{k})$  of the gravitational modes mediating this interaction have ( $k^0 \sim v/r$ ,  $k \sim 1/r$ ), so in order to have manifest power counting it is necessary to Taylor expand the propagator

$$\begin{aligned} G(t, x) &\simeq -i \int \frac{dk_0}{2\pi} \int_{\mathbf{k}} e^{-ik_0 t + i\mathbf{k}\cdot x} \frac{1}{\mathbf{k}^2} \left( 1 + \frac{k_0^2}{\mathbf{k}^2} + \dots \right) \\ &= -i \int_{\mathbf{k}} \delta(t_0) e^{i\mathbf{k}\cdot x} \frac{1}{\mathbf{k}^2} \left( 1 - \frac{\partial_t^2}{\mathbf{k}^2} + \dots \right), \end{aligned} \quad (10)$$

where in the last passage the integral over  $k_0$  has been performed explicitly after trading the  $k_0$  factors for time derivative operators. Note that we did not write any  $i\epsilon$  term in eq. (10) as, in the non-relativistic kinematical region we are interested in here, where the gravitational mode cannot be on-shell, the pole prescription is inessential. The individual particles can also exchange *radiative* gravitons (with  $k_0 \simeq k \sim v/r$ ), but such processes give sub-leading contributions to the effective potential in the PN expansion, and they will be dealt with in subsec. 4.3. In other words we are not integrating out the entire gravity field, but the specific off-shell modes in the kinematic region  $k_0 \ll k$ .

We are aiming at computing an effective action giving the correct action-at-distance, with retardation effects taken into account by the Taylor expansion in eq. (10). After substituting in the effective action (8) the explicit form of the source-gravity coupling one obtains

$$S_{eff} \supset m_{AMB} \int dt \left( 1 + \mathcal{O}(v_1^2) \right) \left( 1 + \mathcal{O}(v_2^2) \right) \int_{\mathbf{k}} \frac{e^{i\mathbf{k}\cdot r}}{\mathbf{k}^2} \left( 1 - \frac{\partial_t^2}{\mathbf{k}^2} + \dots \right). \quad (11)$$



**Figure 3.** Vertex scaling:  

$$\frac{m}{\Lambda} dt d^d k \sim \frac{m}{\Lambda} r^{1-d} v$$



**Figure 4.** A Green function is represented by a propagator, with scaling:  

$$\delta(t)\delta^d(k)/k^2 \sim v r^{1+d}$$



**Figure 5.** Triple internal vertex scaling:  

$$\frac{(k^2, k k_0, k_0^2)}{\Lambda} \delta^d(k) dt (d^d k)^3 \sim \frac{(1, v, v^2)}{r^{1+2d} v \Lambda}$$

Once the time derivatives act on the exponential they will introduce velocity dependent terms in the effective action, so in order to have a consistent calculation at any given order in  $v^2$ , we have to remember the virial theorem, which makes diagrams of the type in fig. 2 also potentially of order  $v^2$  with respect to the leading one in fig. 1. The power counting of diagrams can be made systematic by the rules given in fig. 3,4,5, which can be generalized to higher order interaction vertices.

Intermediate massive object lines, (like the ones in fig. 2) have no propagator associated, as they represent a static source (or sink) of gravitational modes. At the graviton-massive object vertex momentum is *not* conserved, as the graviton momentum is ultra-soft compared to the massive source. E.g. in the diagram of fig. 1, where the massive object emits a single gravitational mode, it recoils by a fractional amount  $dp/p$  roughly given by  $dp/p = \hbar k/(mv) \sim \hbar/L$ , being  $L = mrv$  the macroscopic angular momentum of the binary system. For the phenomenological application we are aiming at,  $\hbar/L \sim 10^{-77} (M/M_\odot)^{-2} (v/0.1)$  is ridiculously small and completely negligible.

Consistently with neglecting any quantum effect, diagrams like the one in fig. 6 will not be considered. Even explicitly restoring  $\hbar$  into the definition of the path integral in eq. (4) to establish the correct dimensions of the exponential term, after evaluating only diagrams at tree level (in the quantum language) all physical result will be  $\hbar$ -independent. According to the standard rules for taking into account powers of  $\hbar$  involved in Feynman diagrams, each vertex brings in an inverse power of  $\hbar$  and each internal line a power of  $\hbar$ , making the quantum scaling of diagram accounted  $\hbar^{I-V} = \hbar^{L-1}$ , using the standard relationship  $L = I - V + 1$  among number of loops  $L$ , vertices  $V$  and propagators  $I$ . Applying this power counting rule to the graph in fig. 6, say, shows that it scales as  $\hbar/L$  with respect to the Newtonian potential, so it is completely negligible. ¶

¶ Note that adopting a quantum field theory description of a second quantized massive particle  $\psi$  coupled to gravity would lead to the same result as here, once the non-relativistic limit is taken, see [30].

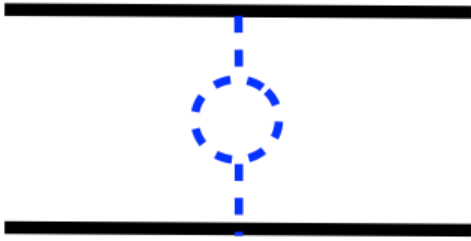


**Figure 6.** Quantum contribution to the 2-body potential.

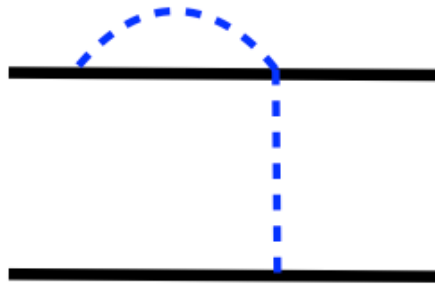


**Figure 7.** Diagram giving a power-law divergent contribution to the mass.

After integrating out the potential graviton we will be left with an effective action where some of the original operators will be renormalized and new, local ones will be generated in infinite numbers (but finite at each PN order), with the coefficients of the generated operators being the *Wilson coefficients*. Note that some graphs will be actually divergent like the one in fig. 7, which gives a divergent contribution to the effective potential

$$fig. 7 \simeq \frac{G_N^2 m_1^3 m_2}{r} \int_{\mathbf{k}} \frac{1}{\mathbf{k}^2}. \quad (12)$$

Actually graphs like this can be consistently discarded, and indeed vanish in dimensional regularization, as an effective theory is not supposed to correctly portrait the full theory at arbitrary high energy scales. Divergences like the one of eq. (12) can be accounted for by shifting the input parameters in the starting Lagrangian (like the mass of the binary constituents), as we are not aiming at *predicting* those parameters, but just take them as inputs (see [31] for a thorough discussion along this line). We shall discuss in the following sections three other kinds of divergence, associated to  $O(3\text{PN})$  gauge artifacts, to long-distance effects and to short-distance (or ultra-violet) incompleteness of the effective theory.

As it is standard in perturbative field theory calculations, diagrams contributing to the effective action are only the *connected* ones, i.e. those in which following Green function's lines all the vertices can be connected.

The effective theory at the orbital case, in the spin-less case, can treat the binary constituents as point-like until 5PN order, as this is the order at which finite size effects come into play, so the theory can be consider ultra-violet (UV) complete up to that order (the finite size spinning effects will be discussed in subsec. 3.2).

In sec. 4 we shall consider the effective action of eq. (1) to describe the binary system as a single extended object coupled to gravity in order to compute observables related to the emission of GWs. The starting point will be the action in eq. (1), where the first two terms will not be responsible for radiation, as at leading order they couple the gravitational modes to the conserved mass monopole and to the total angular momentum.



In order to have full predictive power, the effective theory in terms of the multipole moments at the orbital scale will have to be matched to the theory at the orbital scale in order to express the binary multipoles in terms of individual constituent parameter. It will turn out that in computing the radiation back-reaction on the source at the scale  $\lambda \sim r/v$ , a logarithmic divergence will appear, showing the UV incompleteness already at  $v^3$ , and requiring that the singularity be resolved by considering the theory at the smaller, orbital scale (in the calculation of the emitted flux the incompleteness will appear at  $v^6$  order).

While it is possible to absorb power-divergences into bare parameters of the original Lagrangian, as it is usual in field theory, logarithmic divergences will introduce a spurious dependence on an arbitrary scale  $\mu$ : in order to cancel the  $\mu$  dependence from physical observables, a compensating dependence of the input parameters has to be imposed, leading to a fully classical implementation of the *renormalization group* equation, implying that physical parameters running with  $\mu$  will take different values when probed at different length scale, as it will be explicitly shown in subsec. 4.3.

### 3. Conservative

The conservative dynamics of a binary system involves processes characterized by no incoming nor outgoing radiation: in diagrammatic terms, this means absence of external radiative graviton lines. *Internal* radiative propagators (meaning that the radiation graviton is emitted and then reabsorbed by the system) can in principle be present and indeed appear at 4PN, giving rise to the so called *tail terms* studied in [32, 33, 34]; we will deal with this peculiar effect in subsec. 4.3, while restricting the discussion of this section to diagrams involving potential gravitons only.

The GW length  $\lambda$  thus being irrelevant at this stage, the only scales of the problem are the size of the stars/black holes  $r_s$  and the orbital radius  $r$ . The main goal here is to determine the dynamics of the system as a function of the orbital parameters and of the internal features of the stars, such as mass and spin, and other (like  $c_{E,B}$ ) which appear as Wilson coefficients to be fixed by a matching procedure at the scale  $r_s$ .

The general strategy consists in

- (i) writing down all the relevant vertices of the effective theory and determine their  $v^2$  and  $G_N$  scaling
- (ii) building all the Feynman diagrams which are relevant to the desired PN order
- (iii) computing the Feynman integrals by Taylor expanding potential graviton propagators around  $k_0 = 0$ .

Power-law divergences arising at this point are automatically reabsorbed by dimensional regularization, while the logarithmic divergences appearing for the first time at 3PN can be eliminated by means of a world-line re-parametrization.

The pure gravity sector of the theory can be expanded up to the desired order in terms of the Kaluza-Klein variables introduced in eq. (6). We report here the expansion

up to terms relevant at 4PN + (see also [35] for a derivation):

$$\begin{aligned}
 S_{bulk}^{4PN} \simeq & \int dt d^d x \sqrt{-\gamma} \left\{ \frac{1}{4} \left[ (\vec{\nabla}\sigma)^2 - 2(\vec{\nabla}\sigma_{ij})^2 - (\dot{\sigma}^2 - 2(\dot{\sigma}_{ij})^2) e^{-\frac{c_d\phi}{\Lambda}} \right] \right. \\
 & - c_d \left[ (\vec{\nabla}\phi)^2 - \dot{\phi}^2 e^{-\frac{c_d\phi}{\Lambda}} \right] + \left[ \frac{F_{ij}^2}{2} + (\vec{\nabla}\cdot\vec{A})^2 - \dot{\vec{A}}^2 e^{-\frac{c_d\phi}{\Lambda}} \right] e^{\frac{c_d\phi}{\Lambda}} \\
 & + 2 \frac{\left[ F_{ij} A^i \dot{A}^j + \vec{A}\cdot\dot{\vec{A}}(\vec{\nabla}\cdot\vec{A}) \right] e^{\frac{c_d\phi}{\Lambda}} - c_d \dot{\phi} \vec{A}\cdot\vec{\nabla}\phi}{\Lambda} - c_d \frac{\dot{\phi}^2 \vec{A}^2}{\Lambda^2} \\
 & + 2c_d \left( \dot{\phi} \vec{\nabla}\cdot\vec{A} - \dot{\vec{A}}\cdot\vec{\nabla}\phi \right) + \frac{\dot{\sigma}^{ij}}{\Lambda} \left( -\delta^{ij} A_l \hat{\Gamma}_{kk}^l + 2A_k \hat{\Gamma}_{ij}^k - 2A^i \hat{\Gamma}_{kk}^j \right) \\
 & \left. - \frac{1}{\Lambda} \left( \frac{\sigma}{2} \delta^{ij} - \sigma^{ij} \right) \left( \sigma_{ik}{}^l \sigma_{jl}{}^k - \sigma_{ik}{}^k \sigma_{jl}{}^l + \sigma_{,i} \sigma_{jk}{}^k - \sigma_{ik,j} \sigma^{,k} \right) \right\} \quad (13)
 \end{aligned}$$

All the bulk vertices and propagators needed up to 4PN order can be derived from eq. (13). We write down explicitly the Green function expressions in terms of the space Fourier-transformed variables

$$W_{\mathbf{k}}^a(t) \equiv \int dt d^d x W^a(t, x) e^{-i\mathbf{k}\cdot x} \quad \text{with } W^a = \{\phi, A_i, \sigma_{ij}\} : \quad (14)$$

$$P[W_{\mathbf{k}}^a(t_a) W_{\mathbf{k}'}^b(t_b)] = \frac{1}{2} P^{aa} \delta_{ab} (2\pi)^d \delta^d(\mathbf{k} + \mathbf{k}') \mathcal{P}(\mathbf{k}^2, t_a, t_b) \delta(t_a - t_b), \quad (15)$$

with  $P^{\phi\phi} = -\frac{1}{c_d}$ ,  $P^{A_i A_j} = \delta_{ij}$ ,  $P^{\sigma_{ij} \sigma_{kl}} = -(\delta_{ik} \delta_{jl} + \delta_{il} \delta_{jk} + (2 - c_d) \delta_{ij} \delta_{kl})$  and

$$\mathcal{P}(\mathbf{k}^2, t_a, t_b) = \frac{i}{\mathbf{k}^2 - \partial_{t_a} \partial_{t_b}} \simeq \frac{i}{\mathbf{k}^2} \left( 1 + \frac{\partial_{t_a} \partial_{t_b}}{\mathbf{k}^2} + \frac{\partial_{t_a}^2 \partial_{t_b}^2}{\mathbf{k}^4} \dots \right). \quad (16)$$

As desirable, the three polarization fields  $\phi$ ,  $A$ ,  $\sigma$  do not mix at the quadratic level.

A convenient strategy for building all the Feynman diagrams has two steps (as first done in [36]). At first one determines the shape of the diagram (henceforth called topology), which fixes the powers of  $G_N$  through the following simple rules: a bulk  $n$ -vertex gives  $G_N^{n/2-1}$ , and a matter interaction vertex with  $n$  graviton lines gives  $G_N^{n/2}$ , see e.g. figs. 3,5. Starting from the lowest order topology of fig. 8, all the higher order ones can be generated iteratively by adding a new propagator with one extremum on one of the two stars' word-lines, and the other to any other element (a bulk vertex, a vertex located on the other star's word-line, or in the middle of an other propagator in order to create a new 3-vertex), but not on the same word-line of the first extremum, since as pointed out in sec. 2, topologies involving propagators that start and end on the same star word-line as in fig. 7 do not have to be considered.

Then, any given topology is "filled" with the various  $\phi$ ,  $A$ ,  $\sigma$  field propagators and with the different matter interaction vertices given by eq. 1: these elements determine the powers of  $v$  characterizing the diagram, and thus its PN order. The simplest example of this procedure is depicted in fig. 8.

+  $\hat{\Gamma}_{jk}^i$  is the connection of the purely spatial metric  $\gamma_{ij}$ ,  $F_{ij} \equiv A_{j,i} - A_{i,j}$  and indices must be raised and contracted via the  $d$ -dimensional metric tensor  $\gamma$ ; on the other hand all the spatial derivatives are meant to be simple (not covariant) ones and, when ambiguities might raise, gradients are always meant to act on contravariant fields (so that, for instance,  $\vec{\nabla}\cdot\vec{A} \equiv \gamma^{ij} A_{i,j}$  and  $F_{ij}^2 \equiv \gamma^{ik} \gamma^{jl} F_{ij} F_{kl}$ ).

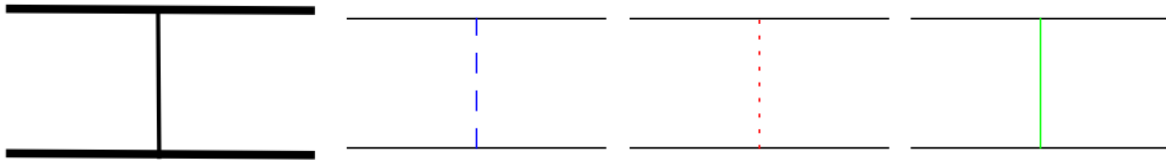


**Figure 8.** The only topology contributing at order  $G_N$ , along with the three diagrams that are derived from it for spin-less objects. The  $\phi$ ,  $A$  and  $\sigma$  propagators are represented respectively by blue dashed, red dotted and green solid lines.

The advantage of this procedure is that each topology is associated with a specific class of Feynman integrals, so that all the diagrams belonging to the same topology can be computed using the same integration strategy. Moreover, topologies which can be split into sub-topologies do not present any new difficulty from the computational point of view because the corresponding amplitudes are given by the product of the sub-topology ones which can thus be evaluated separately.

### 3.1. The spin-less case

Let us consider first the gravity-matter coupling for the non-spinning case and postpone the more complicate spinning case to the next subsection. In this case the finite size of the binary system components does not enter the dynamics until 5PN order (because of the effacement principle discussed in sec. 1), so the gravity-source coupling reduces to the mass monopole term, which can be written as

$$S_{pp} = -m \int d\tau = -m \int dt e^{\phi/\Lambda} \sqrt{\left(1 - \frac{\vec{A} \cdot \vec{v}}{\Lambda}\right)^2 - e^{-c_a \phi/\Lambda} \left(v^2 + \frac{\sigma_{ij}}{\Lambda} v^i v^j\right)}, \quad (17)$$

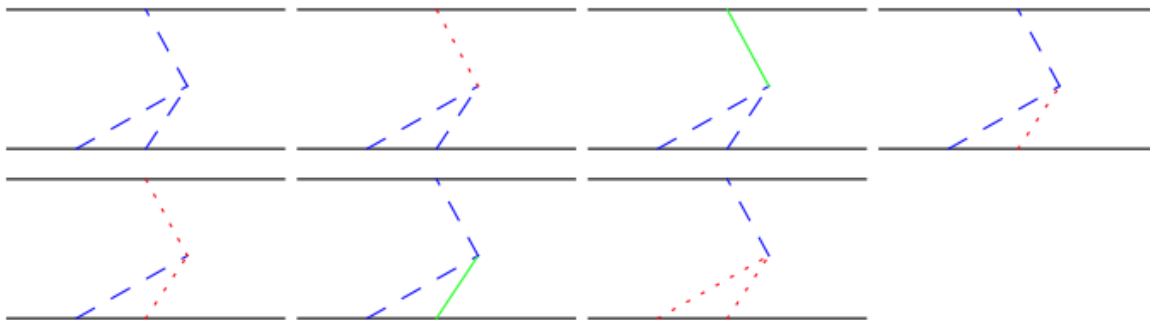
We have now all the elements to complete step (ii), that is to determine all the relevant graphs at a given PN order. The only diagram contributing at Newtonian level is the first one drawn next to the  $\mathcal{O}(G_N)$  topology in fig. 8, because  $\phi$  is the only polarization whose particle interaction vertex does not depend on  $v$  at leading order.

The 1PN diagrams can scale as  $G_N v^2$  or  $G_N^2$ ; in the first category fall the same diagram as before (which has to be computed at  $\mathcal{O}(v^2)$  by expanding the particle interaction vertices and the  $\phi$  propagator according to eqs. (17) and (16), respectively), as well as the second diagram in fig. 8, which carries two powers of  $v$  (one at each particle interaction vertex) at leading order. As to the  $G_N^2$  graphs, one has to consider the new topologies shown in fig. 9 and take the  $v$ -independent part of the Feynman diagrams. Only the diagram with a  $\phi^2$  source-gravity vertex contributes at this PN order while the diagrams involving a triple bulk interaction vertex can be discarded at this order because they carry at least two powers of  $v^*$ . Note that the surviving  $G_N^2$

\* The only diagram that does not pay any  $v$  penalty factor at the particle-gravity interaction vertices



**Figure 9.** The two  $G_N^2$  topologies. The left one affects the dynamics with one diagram at 1PN, one more at 2PN, one more at 3PN and two more at 4PN; the one at the right with 7 diagrams at 2PN, 6 more at 3PN and 5 more at 4PN



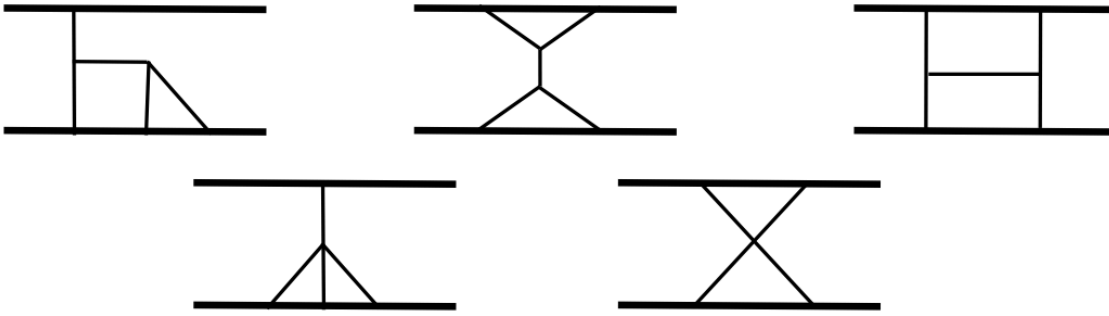
**Figure 10.** The 2PN diagrams coming from the right  $G_N^2$  topology of fig. 9.

diagram at 1PN order is clearly factorisable in terms of two “Newtonian” topologies, so its calculation is straightforward.

At 2PN we have to consider, as well as the previously analyzed diagrams with the appropriate factors of  $v$  from the expansion of the propagators and vertices, also several new diagrams generated by the topologies already considered (see fig. 10 for an example), as well as the ones generated by brand new,  $G_N^3$  topologies. At 2PN, 5 of them are relevant (each one providing a single diagram), 2 of which being merely trivial compositions of three “Newtonian” topologies. The 3 irreducible ones are shown in the upper part of fig. 11. The first computations of the effective 2PN Lagrangian within the EFT framework have been done in [36], using the same Kaluza-Klein decomposition adopted here, and in [37].

We conclude the topology and diagram classification before moving to amplitudes calculation. At 3PN 63 new diagrams have to be considered, and 6 of them come from the two topologies shown in the lower part of fig. 11, which are the only new irreducible topologies needed at this order: in particular, all the 8  $G_N^4$  topologies needed at 3PN are factorisable in terms of simpler ones. The 3PN calculation within the EFT framework has been performed in [38] by means of a semi-automated algorithm thus making the

is the one with three  $\phi$ 's, but the  $\phi^3$  bulk interaction vertex, as it can be seen in eq. (13), carries two time derivatives, giving two powers of  $v$  in the final amplitude.



**Figure 11.** The 5 irreducible  $G_N^3$  topologies: the upper 3 are relevant already at 2PN, while the lower 2 at 3PN. There are other 4  $G_N^3$  topologies not shown here (2 of which are relevant at 2PN and 2 relevant at 3PN) as they are simple products of lower order ones.

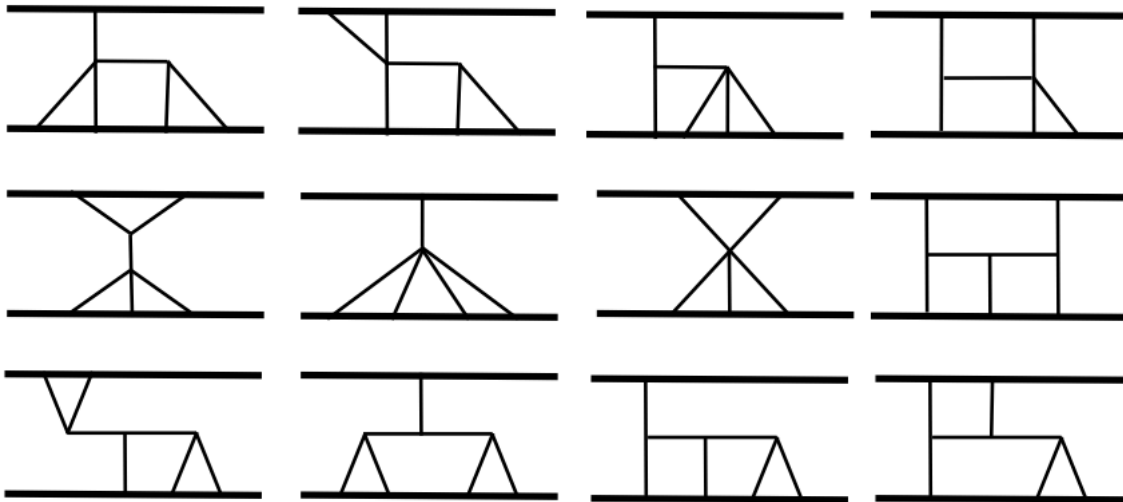


**Figure 12.** The 12 irreducible  $G_N^4$  topologies. They all give contribution to the 4PN dynamics.

EFT technique match what was the state of the art at the time in this sector of the theory.

At 4PN there are 515 new diagrams, variously distributed among the old topologies, new factorisable ones, as well as 12 new irreducible  $G_N^4$  (see fig. 12) topologies and 25  $G_N^5$  ones (fig. 13). Table 1 gives an overview of the topology and diagram counting. The corresponding Lagrangian has been computed for the first time in [39] up to terms of order  $G_N^2$ , a sector which was subsequently also covered in the ADM framework [40, 41].

Coming to step (iii), we have to perform perturbatively the functional integration of eq. (4). As an illustration we take the contribution given by the second diagram of fig. 10. The exponential in the functional integral has to be expanded to the fourth order and the four Lagrangian terms corresponding to the vertices present in the diagram have

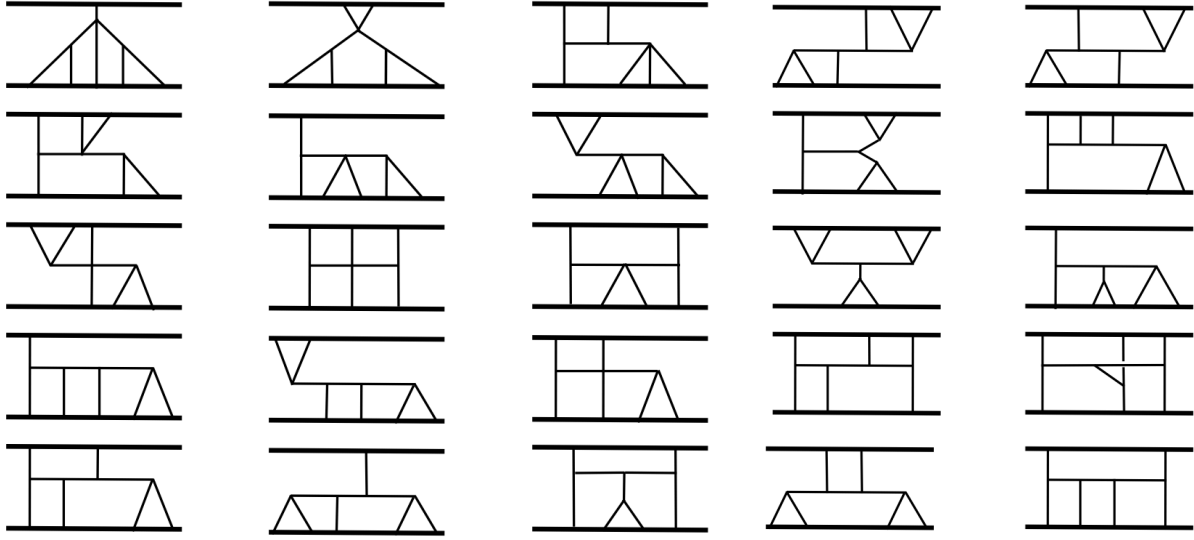


**Figure 13.** The 25 irreducible  $G_N^5$  topologies that contribute at 4PN. Each of them generate just one 4PN diagram. Other 25 4PN diagrams can be obtained from  $G_N^5$  reducible topologies which have not been shown here.

	0PN	1PN	2PN	3PN	4PN		$v^0$	$v^2$	$v^4$	$v^6$
$G$	1					$G$	1	1	1	
$G^2$		1	1			$G^2$	1	8	7	7
$G^3$			5	4		$G^3$	5	48	159	...
$G^4$				8	21	$G^4$	8	299	...	
$G^5$					50	$G^4$	50	...		

**Table 1.** On the left: number of topologies entering at a given PN order. On the right: number of diagrams that start to contribute to the effective action at a given  $G_N$  and  $v$  power, for a total of 595 diagrams up to 4PN. From [38].

to be selected:

$$\begin{aligned}
 iS_{eff} \supset -iV_{ex} \equiv \log \int \mathcal{D}\phi \mathcal{D}A e^{iS_{bulk-free}(\phi, A)} \\
 \frac{1}{2} \int_{t_{1a}, t_{1b}, t_2, t, \vec{x}} \frac{-im_1 \phi_{1a}}{\Lambda} \frac{-im_1 \phi_{1b}}{\Lambda} \frac{im_2 \vec{A}_2 \cdot \vec{v}_2}{\Lambda} \frac{-2ic_d \dot{\phi} \vec{A} \cdot \vec{\nabla} \phi}{\Lambda}, \quad (18)
 \end{aligned}$$

where  $S_{bulk-free}$  is the quadratic part of the bulk gravity action,  $\phi \equiv \phi(t, \mathbf{x})$  and  $\phi_{1a} \equiv \phi(t_{1a}, \vec{x}_1(t_{1a}))$  and so on. Performing the Gaussian integral in the above eq. (18) boils down to substituting pair of like-fields with Green functions like in eq. 8 (indicated below with a contraction, as the procedure is in complete analogy to the Wick theorem in quantum field theory computations):

$$-iV_{ex} = -\frac{m_1^2 m_2 c_d}{\Lambda^4} \int_{t_{1a}, t_{1b}, t_2} 2v_2^i \underbrace{\phi_{1a}} \underbrace{\dot{\phi}_{1b}} \underbrace{\phi^j}_{A_j} \underbrace{A_{2;i}}. \quad (19)$$

Expressing the Green functions in the momentum space via eqs. (14 - 16) one has

$$\begin{aligned}
 -iV_{ex} &= -\frac{m_1^2 m_2}{4c_d \Lambda^4} \int_{t, t_{1a}} \int_{\mathbf{k}, \mathbf{k}_1} \frac{i\delta'(t - t_{1a}) \mathbf{k}_1 \cdot v_2(t)}{\mathbf{k}^2 (\mathbf{k} - \mathbf{k}_1)^2 \mathbf{k}_1^2} e^{i[(\mathbf{k} - \mathbf{k}_1) \cdot x_1(t_{1a}) + \mathbf{k}_1 \cdot x_1(t) - \mathbf{k} \cdot x_2(t)]} \\
 &= -\frac{m_1^2 m_2}{4c_d \Lambda^4} \int_t \int_{\mathbf{k}, \mathbf{k}_1} \frac{i\mathbf{k}_1 \cdot v_2(t)}{\mathbf{k}^2 (\mathbf{k} - \mathbf{k}_1)^2 \mathbf{k}_1^2} i(\mathbf{k} - \mathbf{k}_1) \cdot v_1(t) e^{i\mathbf{k} \cdot \mathbf{r}}. \tag{20}
 \end{aligned}$$

A look at the structure of the denominator tells us that the complexity of this diagram (and of all the diagrams derived from the same topology) is equivalent to 1-loop diagrams in quantum field theory (QFT); indeed, this amplitude can be easily evaluated using standard textbook formulae and taking the limit  $d \rightarrow 3$  (in this case the amplitude is finite in dimensional regularization, so  $d = 3$  could have been set from the beginning), thus bringing to the following term of the 2PN action

$$V_{ex} = -\int_t \frac{G_N^2 m_1^2 m_2}{r^2} [v_1^r v_2^r - v_1 \cdot v_2], \quad v_i^r \equiv \frac{r \cdot v_i}{r}. \tag{21}$$

Naturally, the same diagram contributes also to higher PN's, and the corresponding amplitude is obtained as above with the caution of including the appropriate orders in the  $v$  expansion of  $S_{pp}$  from eq. (17) and in the propagators expansions, eq. (16). The latter may generally bring more and more  $\mathbf{k}, \mathbf{k}_1$  terms in the integrand numerator thus making the evaluation more lengthy, but as the general structure of the denominator does not change, the complexity of momentum integrals remains still comparable to 1-loop ones.

All amplitudes can be expressed in terms of (eventually complicated) spatial momentum integrals along the same lines. The actual evaluation strategy of the integrals depends on the topology and, as we have seen, all the topologies up to  $G_N^2$  can be computed by directly applying standard textbook formulae. Generally, a  $G_N^{(n+1)}$  irreducible topology is expected to involve momentum integrals equivalent to  $n$ -loops QFT diagrams, but a more careful inspection shows that the situation is actually more favorable. For instance, four of the five irreducible  $G_N^3$  topologies in fig. 11 involve *nested* loops integrations, that is integrals where at least one  $\mathbf{k}_a$  appear just twice in the denominator: in this case this variable can be integrated out immediately as in the 1-loop case, and the result of the partial integration is, in the  $G_N^3$  case, easily integrable in terms of the remaining momentum variables. The only apparent exception to this rule is the H-shaped topology in fig. 11, but an appropriate use of Integration by Parts techniques provide the following useful relation

$$\begin{aligned}
 I(\alpha, \beta, \gamma, \delta, \epsilon) &\equiv \int_{\mathbf{k}_1, \mathbf{k}_2} [\mathbf{k}_1^{2\alpha} (\mathbf{k} - \mathbf{k}_1)^{2\beta} \mathbf{k}_2^{2\gamma} (\mathbf{k} - \mathbf{k}_2)^{2\delta} (\mathbf{k}_1 - \mathbf{k}_2)^{2\epsilon}]^{-1} \\
 &= \frac{\gamma [I(\alpha-, \gamma+) - I(\epsilon-, \gamma+)] + \delta [I(\beta-, \delta+) - I(\epsilon-, \delta+)]}{2\epsilon + \gamma + \delta - d} \tag{22}
 \end{aligned}$$

with the notation  $I(\alpha-, \gamma+) \equiv I(\alpha - 1, \beta, \gamma + 1, \delta, \epsilon)$ , by means of which the integrals of this topology can be reduced to nested loops ones. Thus, the  $G_N^3$  sector does not present new conceptual difficulties with respect to the  $G_N^2$  one, although the computational challenge becomes relevant at high PN because of the high number of diagrams involved, see tab. 1, and of the appearance of more and more  $\mathbf{k}_a$  factors in the numerators.

The situation is somehow similar in the  $G_N^4$  case, as it turns out that the topologies of this order involve, in the most difficult case, 3-loops integrals which are either nested or reducible through integrations by parts to integrals like the one in eq. (22). Consequently one has the remarkable result that all the topologies up to  $G_N^4$  are basically tractable in terms of 1-loop equivalent QFT diagrams, see also [42] for related work.

At  $G_N^5$  however things change, for two reasons: first, the use of integration by parts becomes more complicated and substantially intractable by hand. This problem can be overcome by using automated reduction packages which are routinely used in particle physics multi-loop calculations, see e.g. [43]. Second, and more important, the “miracle” according to which everything could be ultimately reduced to 1-loop integrals does not take place anymore: in the worst cases, that is for the topologies in  $(row, column) = (3, 2)$  and  $(4, 5)$  in fig. 13, one is left even after integration by parts with integrals equivalent to a 4-loop mass-less QFT diagram, which has to be evaluated in  $d \sim 3$  by means of *ad hoc* techniques [44]. A possibly more efficient way to reorganize the diagrams have been proposed in [45], while a radically different computational method has been recently suggested in [46].

Starting from 3PN, divergences appear in the form of  $(d - 3)$  poles:

$$\mathcal{L}_{pole}^{3PN} = -\frac{11G_N^2 m_1^2 m_2}{2(d-3)} [a_1^2 + 2a_1 \cdot a_2] + \frac{11G_N^3 m_1^2 m_2^2}{3(d-3)} a_1^r + (1 \leftrightarrow 2). \quad (23)$$

This divergence is not due to a short-distance incompleteness of the effective field theory approach, and it has been found in all the past treatments at 3PN with different kind of regularisations, see [47, 48, 49, 50, 51]. Since a Lagrangian is not an observable we can allow divergent terms in it as long as any relation among observables is given by finite expressions: e.g. this singularity does not appear in the expression for  $E(\omega)$  relating the energy  $E$  of the system to the orbital angular velocity  $\omega$ . It is however more practical to deal with a finite quantity also at the Lagrangian level and this can be obtained at 3PN by means of the following word-line re-parametrization:

$$\vec{x}_{1,2} \rightarrow \vec{x}_{1,2} + \frac{G_N^2 m_{1,2}^2}{3} \vec{a}_{1,2}, \quad (24)$$

see [11] and [38] for details.

The EFT approach allowed us to compute for the first time the dynamics at 4PN up to  $\mathcal{O}(G_N^2)$  (while some sectors at higher  $G_N$  order have been recently covered in the ADM framework [41]). We write here the expression of the energy in the center of mass frame, addressing to [39] for other details:

$$\begin{aligned} E^{4PN} = & \frac{9\mu v^{10}}{256} (7 - 121\nu + 785\nu^2 - 2254\nu^3 + 2415\nu^4) \\ & + \frac{GM\mu}{128r} [v^8 (525 - 4011\nu + 9507\nu^2 - 714\nu^3 - 15827\nu^4) \\ & - 4v^6 v^{r^2} (147 - 369\nu - 1692\nu^2 + 4655\nu^3) \nu \\ & + 18v^4 v^{r^4} (3 + 54\nu - 374\nu^2 + 539\nu^3) \nu \\ & + 20v^2 v^{r^6} (5 - 50\nu + 148\nu^2 - 119\nu^3) \nu \end{aligned}$$



$$\begin{aligned}
 & -35v^{r8} \left(1 - 7\nu + 14\nu^2 - 7\nu^3\right) \nu] \\
 & + \frac{G^2 M^2 \mu}{1920 r^2} \left[15v^6 \left(2300 - 4489\nu + 10258\nu^2 - 16478\nu^3 - 7800\nu^4\right) \right. \\
 & + 15v^4 v^{r2} \left(120 - 5983\nu - 25990\nu^2 + 37022\nu^3 + 22760\nu^4\right) \\
 & + 5v^2 v^{r4} \left(5347 + 77860\nu - 21072\nu^2 - 25920\nu^3\right) \nu \\
 & \left. - 3v^{r6} \left(4771 + 36880\nu + 5440\nu^2 - 4800\nu^3\right) \nu\right] + \mathcal{O}(G_N^3), \quad (25)
 \end{aligned}$$

with the symmetric mass ratio given by  $\nu \equiv m_1 m_2 / M^2$ .

Specializing then to circular orbits, that allows to express both  $v$  and  $G_N M / r$  in terms of  $x \equiv (G_N M \omega)^{2/3}$ , at 4PN one has

$$\begin{aligned}
 E(x)|_{4PN} = & -\mu \frac{x^5}{2} \left[ -\frac{3969}{128} + \left( \frac{448}{15} \log(x) - \frac{123671}{5760} + \frac{9037}{1536} \pi^2 + \frac{1792}{15} \log 2 + \frac{896}{15} \gamma \right) \nu + \right. \\
 & \left. + \left( -\frac{498449}{3456} + \frac{3157}{576} \pi^2 \right) \nu^2 + \frac{301}{1728} \nu^3 + \frac{77}{31104} \nu^4 \right], \quad (26)
 \end{aligned}$$

where  $\gamma \simeq 0.577\dots$  is the Eulero-Mascheroni constant. Eq. (25), together with inputs from Lorentz invariance of the 3PN Lagrangian, allows to derive the  $\nu^3$  and  $\nu^4$  term in the above eq. (26), first obtained in [40], while the  $\nu^2$  term has been obtained more recently in [41]. The term linear in  $\nu$  has been obtained within the extreme mass ratio limit approach in [52, 53], and its non-logarithmic part has been analytically computed in [54]. We shall discuss in subsec. 4.3, how the logarithmic piece can be derived from radiation reaction computation. The  $\nu$ -independent part can be derived from the Schwarzschild result.

### 3.2. Spin

EFT methods are giving a relevant contribution to the study of the spin sector of compact binary systems: the next-to leading order (NLO) dynamics with a quadratic dependence on the stars' spins has been computed for the first time in [55, 56, 57], triggering a renewed attention on such sector and a healthy competition with more traditional approaches, which led to the confirmation of the new results and even to the extension to NNLO for the  $S_1 S_2$  potential [58, 59] and for spin-orbit [58, 60, 61, 62].

As the spin of a compact star and the lowest-order spin-orbit and spin-spin interactions scale respectively like

$$S \sim M v_{\text{rot}} R_s, \quad V_{SO} \sim \frac{G_N M}{r^2} v \cdot S, \quad V_{S^2} \sim \frac{G_N}{r^3} S_1 \cdot S_2, \quad (27)$$

one deduces that the lowest order (LO) spin orbit potential is a 1.5PN term for maximally rotating objects ( $v_{\text{rot}} \sim 1$ ), while the LO spin-spin interaction starts at 2PN.

Spin interactions in general relativity are introduced by means of the tetrad  $e_a^\mu$  (for a more detailed discussion, see the papers cited in this section and [63, 64, 65]). which transforms the metric into a locally free-falling (and locally Lorenz-invariant) frame:

$$g_{\mu\nu} e_a^\mu e_b^\nu = \eta_{ab}. \quad (28)$$

If such frame is also chosen to be co-rotating with the spinning body, the tetrad geodesic variation is locally a rotation with generalized angular velocity given by

$$\frac{de^{a\mu}}{d\tau} \equiv u^\rho e_{;\rho}^{a\mu} = \Omega_\nu^\mu e^{a\nu} \implies \Omega^{\mu\nu} = e_a^\mu \frac{de^{a\nu}}{d\tau} = -\Omega^{\nu\mu}, \quad (29)$$

where  $u^\rho$  is the four velocity of the spinning body. Local coordinate, Lorentz and parametrization invariances require the Lagrangian to be made of invariant contractions of  $\Omega^{\mu\nu}$ ,  $u^\rho$  and eventually of the local curvature tensors, but do not unambiguously fix its form even in the case of flat space-time. However it turns out that if one neglects finite-size effects, the variation of any possible Lagrangians w.r.t. to the spinning body local position and tetrad, when expressed in terms of the conjugate momenta  $p^\mu = \frac{\delta\mathcal{L}}{\delta u_\mu}$  and  $S^{\mu\nu} = \frac{\delta\mathcal{L}}{\delta\Omega_{\mu\nu}}$ , gives the same (Mathisson-Papapetrou) equations of motion:

$$\begin{aligned} \frac{dp^\mu}{d\tau} &= -\frac{1}{2}R_{\mu\nu\rho\sigma}u^\nu S^{\rho\sigma}, \\ \frac{dS^{\mu\nu}}{d\tau} &= p^\mu u^\nu - p^\nu u^\mu. \end{aligned} \quad (30)$$

Since the spin is related to the conjugate momentum  $S^{\mu\nu}$  rather than to the fundamental tetrad variables themselves, it is actually more convenient to work with a functional that behaves as an Hamiltonian with respect to the spin, while remaining a Lagrangian with respect to the body position  $x^\mu$ . Such functional is called a Routhian and one can verify that the following form involving the spin connection  $\omega_\mu^{ab} \equiv e^{b\nu} e_{\nu;\mu}^a$

$$\mathcal{R}_0 = -m\sqrt{-u^2} - \frac{1}{2}S_{ab}\omega_\mu^{ab}u^\mu, \quad (31)$$

gives exactly the Mathisson-Papapetrou equations by means of

$$\frac{\delta}{\delta x^\mu} \int dt R = 0, \quad \frac{dS^{ab}}{d\tau} = \{\mathcal{R}, S^{ab}\}, \quad (32)$$

once the following Poisson bracket is taken into account:

$$\{S^{ab}, S^{cd}\} = \eta^{ac}S^{bd} + \eta^{bd}S^{ac} - \eta^{ab}S^{cd} - \eta^{cd}S^{ab}. \quad (33)$$

The antisymmetric tensor  $S^{\mu\nu}$  (which appears above through its locally flat-frame components  $S^{ab} \equiv S^{\mu\nu} e_\mu^a e_\nu^b$ ) is the generalized spin of the body and it contains redundant degrees of freedom. The redundancy corresponds to the ambiguity related the choice of a reference world-line inside the body. One can reduce from 6 to the 3 degrees of freedom needed to describe an ordinary spin vector by imposing the Spin Supplementary Condition (SSC), which relates the vector  $S^{0i}$  to the physical spin components  $S^i \equiv \varepsilon^{ijk} S_{jk}$ . There is not a unique way to impose such condition and the so-called covariant SSC

$$S^{\mu\nu} p_\nu = 0 \quad (34)$$

will be taken here. The requirement of SSC conservation along the world line gives the following relation:

$$p^\mu = m \frac{u^\mu}{\sqrt{-u^2}} + \frac{1}{2m} R_{\nu\beta\rho\sigma} S^{\mu\nu} S^{\rho\sigma} \frac{u^\beta}{\sqrt{-u^2}} + \mathcal{O}(R_{\nu\beta\rho\sigma}^2), \quad (35)$$

where the first term in the r.h.s. is SSC-independent and gives the familiar dynamics for a non spinning body.

Such relation can be enforced at the level of the Routhian by adding

$$\mathcal{R}_{SSC} \equiv -\frac{1}{2m} R_{abcd} S^{cd} S^{ae} \frac{u^b u^e}{\sqrt{-u^2}} + \mathcal{O}(R_{\nu\beta\rho\sigma}^2) \quad (36)$$

at the l.h.s. of eq. (31).

It should be remarked that imposition of the SSC implies  $S^{0i} \sim S^{ij} v_j$  thus providing different scalings for the different components of the spin tensor. Being an algebraic constraint, the SSC can be imposed by direct replacement of  $S^{0i}$  indifferently at the level of the fundamental Routhian or in the effective potential or in the equations of motion: the second option will be followed here because it simplifies intermediate calculations, at the price however of some loss of transparency in the results, which will not have a transparent physical interpretation until the SSC will be enforced.

Spin-induced finite size-effects become relevant much before than in the spin-less case; the lowest order of these effects is the spin-induced quadrupole moment, which can be taken into account by the following Routhian term

$$\mathcal{R}_{fs} \equiv \frac{C_{ES^2}}{2m} \frac{E_{ab}}{\sqrt{-u^2}} S_c^a S^{cb}, \quad (37)$$

where  $E_{ab}$  is the electric part of the Weyl tensor, and  $C_{ES^2} = 1$  for black holes, while it has to be fixed via a matching procedure in the non-BH case. This term gives an effective contribution to the  $I_{ij} E_{ij}$  interaction in eq. (1) already at 2PN order.

The spin-dependent part of the Routhian can be expressed as follows in terms of the Kaluza-Klein fields:

$$\begin{aligned} \mathcal{R} &\supset S^{ij} \left\{ \frac{1}{4} F_{ij} (1 + 4\phi + 8\phi^2) + \frac{1}{2} A_j \phi_{,i} [1 + 3\phi] + \frac{1}{2} A_j v_i \dot{\phi} + \frac{1}{4} F_{jk} \sigma_i^k + \frac{1}{8} A_i \dot{A}_j \right. \\ &+ [A_j A_{i,k} - 2F_{ij} A_k + 2A_i A_{k,j}] \frac{v^k}{8} + \phi_{,j} v_i + \frac{1}{2} \sigma_{jk,i} v^k + \frac{1}{2} \sigma_{ik} (\phi_{,j} v^k + \phi^k v_j) \left. \right\} \\ &+ S^{0i} \left\{ \frac{1}{2} \dot{A}_i (1 + 3\phi) + \left[ \phi_{,i} - \frac{1}{4} F_{ij} v^j \right] (1 + 2\phi) + \frac{1}{2} \dot{\sigma}_{ij} v^j + \frac{1}{4} F_{ij} A^j - \frac{3}{2} A_k v^k \phi_{,i} \right. \\ &+ \frac{1}{2} A^k \phi_{,k} v_i + \frac{1}{2} (\phi A_{i,k} - A_i \phi_{,k}) v^k + \frac{1}{2} A_i \dot{\phi} - \frac{1}{2} \sigma_{ij} \phi_{,j} \left. \right\} + \frac{1}{2m} S^{jk} S^{il} A_{k,ij} v_l \\ &+ \frac{C_{ES^2}}{2} \left\{ \left[ (\vec{\nabla} \phi)^2 + \vec{a} \cdot \vec{\nabla} \phi \right] (S^{kl})^2 + 2S^{0k} S^{jk} \phi_{,ij} v^i + S^{0i} S^{0j} \phi_{,ij} \right. \\ &+ \left. \left[ \phi_{,ij} (1 + 2\phi) + 2\phi_{,i} \phi_{,j} + A_{l,ij} v^l + 2\phi_{,i} v_j + \frac{3}{2} \phi_{,ij} v^2 + 2\phi_{,il} v_j v^l + \frac{1}{4} F_{ik} F_{jk} \right] S^{ik} S^{kj} \right\}, \quad (38) \end{aligned}$$

where  $d$  has been set to 3 as all the results obtained so far from this Routhian are at most next-to-next-to leading order and thus finite. By analogy to the spin-less case, (gauge-dependent) divergences are expected to appear at next-to-next-to-next-to leading order, corresponding to 4.5PN for spin orbit, and to 5PN for spin-quadratic interactions.

The determination of the effective potential proceeds along the same lines of the spin-less case, with the new Feynman rules dictated by (38). Spin insertions in the



**Figure 14.** Graphs contributing at leading order to the Spin-Orbit potential.

diagrams introduce PN penalty factors, making the integrals to be computed easier than the ones without spin at the same PN order, while the physical interpretation of the results is made less transparent in the spinning case.

To illustrate the latter point, let us consider the lowest order spin-orbit interaction. According to the scaling rules (and reminding that  $S^{0i} \sim v_j S^{ij}$ ), the effective potential is a 1.5 PN contribution that can be derived from the two graphs in fig. 14 and their mirror images. The computation is straightforward and gives

$$V_{LO}^{SO} = -\frac{G_N m_2}{r^3} \left[ \vec{S}_1 \cdot (\vec{v}_1 - 2\vec{v}_2) \wedge \vec{r} + S_1^{0i} r_i \right] + (1 \leftrightarrow 2). \quad (39)$$

The non-physical degrees of freedom represented by  $S^{0i}$  must now be eliminated through a SSC, as for instance the covariant one in eq. (34). By taking such condition at leading order in  $v$  one gets

$$V_{LO}^{SO} = -2 \frac{G_N m_2}{r^3} \vec{S}_1 \cdot \vec{v} \wedge \vec{r} + (1 \leftrightarrow 2), \quad (40)$$

which however does not correspond to the canonical result, see e.g. [66]:

$$V_{LO}^{SO} = 2 \frac{G_N m_2}{r^3} \vec{S}_1 \cdot \vec{v} \wedge \vec{r} + \frac{1}{2} \vec{S}_1 \cdot \vec{v}_1 \wedge \vec{a}_1 + (1 \leftrightarrow 2). \quad (41)$$

The mismatch does not lead to any difference in physical observables, as it can be cured by means of the following spin-dependent coordinate transformation at the Lagrangian level

$$\vec{x}_{1,2} \rightarrow \vec{x}_{1,2} + \frac{1}{2m_{1,2}} \vec{S}_{1,2} \wedge \vec{v}_{1,2}. \quad (42)$$

Alternatively, an expression matching exactly eq. (41) may be obtained by imposing the so-called Newton-Wigner SSC,  $S^{\mu\nu} (p_\nu + m e_\nu^0) = 0$ , as well as the Newtonian equations of motion for the accelerations [67].

To summarize, the choice of working with  $S^{0i}$  at the effective potential level makes the results formally SSC-dependent, but the difference vanishes on observables. Clearly when going at higher PN orders one should not forget to include effects coming from the higher order terms in the SSC relation eventually inherited from lower PNs. An alternative procedure is to impose the SSC directly at the level of

the fundamental Routhian, a strategy which however brings unnecessary complications in the intermediate steps of the calculation. Whatever choice is made, one is left with some difficulties in comparing results derived within different approaches, like the EFT method and the ADM approach (a problem somehow addressed for instance in [68]). Not surprisingly, such difficulties become computationally more relevant at higher post-Newtonian order, as is the case for the  $S_1S_2$  4PN sector, where a full comparison between the two approaches has not yet been carried on.

#### 4. Radiation

In the previous section we have shown how to obtain an effective action à la Fokker describing the dynamics of a binary system at the orbital scale  $r$  in which gravitational degrees of freedom have been integrated out, resulting in a series expansion in  $v^2$ , as in a conservative system odd powers of  $v$  are forbidden by invariance under time reversal.

The gravitational tensor in 3+1 dimensions has 6 physical degrees of freedom (10 independent entries of the symmetric rank 2 tensor in 3+1 dimensions minus 4 gauge choices): 4 of them are actually constrained, non radiative physical degrees of freedom, responsible for the gravitational potential, and the remaining 2 are radiative, or GWs.

In order to compute interesting observables, like the average energy flux emitted by or the radiation reaction on the binary system, it will be useful to “integrate out” also the radiative degrees of freedom, with characteristic length scale  $\lambda = r/v$ , as it will be shown in the next subsections.

We aim now at writing the coupling of an extended source appearing in eq. (1) in terms of the energy momentum tensor  $T^{\mu\nu}(t, x)$  moments. Here we use  $T^{\mu\nu}$ , as in [69], to denote the term relating the effective action  $\mathcal{S}_{1g}$  relative to the single graviton emission

$$\mathcal{S}_{1g} \propto \int dt d^d x T^{\mu\nu}(t, x) h_{\mu\nu}(t, x), \quad (43)$$

to the gravitational mode generically denoted by  $h_{\mu\nu}$ . With this definition  $T^{\mu\nu}$  receives contribution from both matter and the gravity *pseudo-tensor* appearing in the traditional GR description of the emission processes.

Given that the variation scale of the energy momentum tensor and of the radiation field are respectively  $r_{source}$  and  $\lambda$ , by Taylor-expanding the standard term  $T_{\mu\nu}h^{\mu\nu}$

$$\sum_n \frac{1}{n!} \partial_1 \dots \partial_n h_{\mu\nu}(t, x) \Big|_{x=0} \int d^d x' T^{\mu\nu}(t, x') x'_1 \dots x'_n, \quad (44)$$

we obtain a series in  $r_{source}/\lambda$ , which for binary systems gives  $r_{source} = r \ll \lambda = r/v$ .

The results of the integral in eq. (44) are source moments that, following standard procedures not exclusive of the effective field theory approach described here, are traded for mass and velocity multipoles. For instance, the integrated moment of the energy momentum tensor can be traded for the mass quadrupole

$$Q_{ij}(t) \equiv \int d^d x T_{00}(t, x) x_i x_j, \quad (45)$$

by repeatedly using the equations of motion under the form  $T_{\mu\nu}{}^{,\nu} = 0$ :

$$\begin{aligned} \int d^d x [T_{0i}x_j + T_{0j}x_i] &= \int d^d x T_{0k} (x_i x_j)_{,k} \\ &= - \int d^d x T_{0k,k} x_i x_j \\ &= \int d^d x \dot{T}_{00} x_i x_j = \dot{Q}_{ij} \end{aligned} \quad (46)$$

$$\begin{aligned} 2 \int d^d x T_{ij} &= \int d^d x [T_{ik} x_{j,k} + T_{kj} x_{i,k}] \\ &= \int d^d x [\dot{T}_{0i}x_j + \dot{T}_{0j}x_i] \\ &= \int d^d x \ddot{T}_{00}x_i x_j = \ddot{Q}_{ij}. \end{aligned} \quad (47)$$

The above equations also show that as for a composite binary system  $T_{00} \sim O(v^0)$ , then  $T_{0i} \sim O(v^1)$  and  $T_{ij} \sim O(v^2)$ .

Taking as the source of GWs the composite binary system, the multipole series is an expansion in terms of  $r/\lambda = v$ , so when expressing the multipoles in terms of the parameter of the individual binary constituents, powers of  $v$  have to be tracked in order to arrange a consistent expansion. At lowest order in the multipole expansion and at  $v^0$  order

$$\mathcal{S}_{ext}|_{v^0} = \frac{1}{\Lambda} \int dt d^d x T_{00}|_{v^0} \phi = \frac{M}{\Lambda} \int dt \phi, \quad (48)$$

where in the last passage the explicit expression

$$T_{00}(t, x)|_{v^0} = \sum_A m_A \delta^{(3)}(x - x_A(t)), \quad (49)$$

has been inserted. At order  $v$  the contribution from the first order derivative in  $\phi$  have to be added the contribution of  $T_{\mu\nu}|_v$ , which gives

$$\mathcal{S}_{ext}|_v = \frac{1}{\Lambda} \int dt d^d x (T_{00}|_{v^0} x_i \phi_{,i} + T_{0i}|_v A_i), \quad (50)$$

with

$$T_{0i}(t, x)|_v = \sum m_A v_{Ai} \delta^{(3)}(x - x_A(t)), \quad (51)$$

and neither  $T_{00}$  nor  $T_{ij}$  contain terms linear in  $v$ . Since the total mass appearing in eq. (48) is conserved (at this order) and given that in the center of mass frame  $\sum_A m_A x_{Ai} = 0 = \sum_A m_A v_{Ai}$ , there is no radiation up to order  $v$ . From order  $v^2$  on, following a standard procedure, see e.g. [18], it is useful to decompose the source coupling to the gravitational fields in irreducible representations of the  $SO(3)$  rotation group, to obtain

$$\begin{aligned} \mathcal{S}_{ext}|_{v^2}^{\mathbf{1}} &= -\frac{1}{2} \int dt d^d x T_{0i}|_v x_j (A_{i,j} - A_{j,i}), \\ \mathcal{S}_{ext}|_{v^2}^{\mathbf{0+2}} &= \frac{1}{2} \int dt Q_{ij}|_{v^0} \left( \ddot{\sigma}_{ij} - 2\dot{\phi}_{,ij} - \frac{2}{d-2} \ddot{\phi} \delta_{ij} - \dot{A}_{i,j} - \dot{A}_{j,i} \right), \end{aligned} \quad (52)$$

where eqs. (46,47) and integration by parts have been used,  $\mathbf{0}, \mathbf{1}, \mathbf{2}$  stand for the scalar, vector and symmetric-traceless representations of  $SO(3)$ , and

$$Q_{ij}|_{v^n} = \int d^d x T_{00}|_{v^n} x_i x_j. \quad (53)$$

The  $\mathbf{0} + \mathbf{2}$  term in eq. (52) reproduces at linear order the  $E_{ij}$  term in eq. (1), allowing to identify  $I_{ij}$  with  $Q_{ij}$  at leading order.

The  $\mathbf{1}$  part matches the second term in eq. (1), and it is not responsible for radiation as it couples  $A_i$  to the conserved angular momentum. In order to simplify the calculation, we work from now on in the transverse-traceless (TT) gauge, in which the only relevant radiation field is the traceless and transverse part of  $\sigma_{ij}$ . The presence of the other gravity polarizations is required by gauge invariance.

Discarding all fields but the TT-part of the  $\sigma_{ij}$  field, at order  $v^3$  one has

$$S_{ext}|_{v^3} = \int dt d^d x T_{ij}|_{v^2} x_k \sigma_{ij,k} \quad (54)$$

and using the decomposition [18]

$$\begin{aligned} \int d^d x T_{ij} x_k &= \frac{1}{6} \int d^d x \ddot{T}_{00} x^i x^j x^k \\ &+ \frac{1}{3} \int d^d x \left( \dot{T}_{0i} x_j x_k + \dot{T}_{0j} x_i x_k - 2\dot{T}_{0k} x_i x_j \right), \end{aligned} \quad (55)$$

we can re-write

$$S_{ext}|_{v^3} = \int dt \left( \frac{1}{6} Q_{ijk} E_{ij,k} - \frac{2}{3} P_{ij} B_{ij} \right) \quad (56)$$

where

$$P_{ij} = \int d^d x \left( \epsilon_{ikl} T^{0k} x^l x_j + \epsilon_{jkl} T^{0k} x^l x_i \right), \quad (57)$$

and

$$Q_{ijk} = \int d^d x T_{00} x_i x_j x_k, \quad (58)$$

allowing to identify  $J_{ij} \leftrightarrow P_{ij}$  and  $I_{ijk} \leftrightarrow Q_{ijk}$  at leading order.

At  $v^4$  order the  $T_{ij} x^k x^l \sigma_{ij,kl}$  term, beside giving the leading hexadecapole term (or  $2^4$ -th-pole), also gives a  $v^2$  correction to the leading quadrupole interaction  $I_{ij} E^{ij}$ , which can be written as

$$S_{ext}|_{v^4} \supset \int d^{d+1} x \left[ T_{00}|_{v^2} + T_{kk}|_{v^2} - \frac{4}{3} \dot{T}_{0k}|_v x^k + \frac{11}{42} \ddot{T}_{00}|_{v^0} x^2 \right] \left( x^i x^j - \frac{\delta_{ij}}{d} x^2 \right) E_{ij} \quad (59)$$

For the systematics at higher orders see [70] or the standard textbook [18].

#### 4.1. Matching between the radiation and the orbital scale

In the previous subsection we have spelled out the general expression of the effective multipole moments in terms of the energy-momentum tensor moments. However we have only used two ingredients from the specific binary problem

- $T_{00} \sim mv^0$
- the source size is  $r$  and the length variation of the background is  $\lambda \sim r/v$ .

Now we are going to match the coefficients appearing in eq. (1) with the parameters of the specific theory at the orbital scale.

At leading order  $Q_{ij}|_{v^0} = \sum_A m_A x_{Ai} x_{Aj}$  and the  $v^2$  corrections to  $T_{00}$  can be read from diagrams in figs. 15,16. Such diagrams account for the pseudo-energy momentum

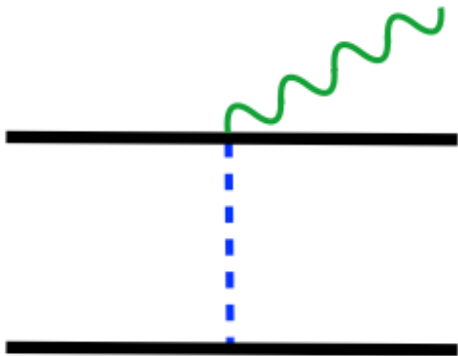


**Figure 15.** Graph dressing  $T_{00}$  at  $v^2$  order.

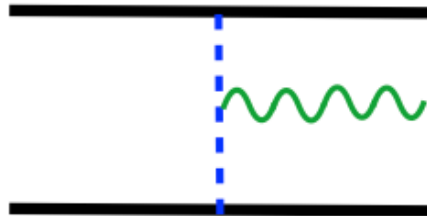


**Figure 16.** Graph dressing  $T_{ij}$  at leading order. The external radiation graviton does not carry momentum but it is Taylor expanded according to eq. (44).

tensor of the gravitational field and are obtained by computing the effective action with the *background field method*, and picking the term in the resulting effective action linearly coupled to the background gravity field [12].

As  $\phi$  couples to  $T_{00} + T_{kk}/(d-2)$  and  $\sigma_{ij}$  to  $T_{ij}$ , from the diagrams one obtains $\ddagger$

$$\begin{aligned} \int d^d x \left( T_{00} + \frac{1}{d-2} T_{kk} \right) \Big|_{v^2} &= \sum_A \frac{d}{2(d-2)} m_A v_A^2 - g(d) \sum_{B \neq A} \frac{G_N m_A m_B}{r^{d-2}}, \\ \int d^d x T_{kk} \Big|_{v^2} &= \sum_A \frac{1}{2} m_A v_A^2 - \frac{d-2}{2} g(d) \sum_{B \neq A} \frac{G_N m_A m_B}{r^{d-2}}, \end{aligned} \quad (60)$$

where  $g(d) = (d-2)\Gamma(d/2-1)/[\pi^{d/2-1}2^{d-4}(d-1)]$ . The calculation can be iterated for all higher multipoles, and it does not contain any fundamental difference if framed within the effective field theory approach or traditional methods.

#### 4.2. Spin contribution to the source moments

In the case of spinning individual sources, in order to add the spin contributions to the energy-momentum tensor we start from the spin-world-line term in eq. (31) to obtain

$$\sqrt{-g} T^{\mu\nu}(t, x) = \frac{1}{2} \sum_A \partial_\alpha \delta^{(3)}(x - x(t)) (S_A^{\mu\alpha} u_A^\nu + S_A^{\nu\alpha} u_A^\mu), \quad (61)$$

$\ddagger$  Note that since only  $\int T_{kk}$  is needed, and not  $T_{kk}$  itself, it could have been computed from eq. (47) instead of from the diagram in fig. 16.



from which it is possible to derive [71] the leading order energy momentum tensor components linear in the spins:

$$\begin{aligned}
 T^{00}(t, \mathbf{k})|_{S^1} &= \sum S_A^{0i} i\mathbf{k}^i e^{-i\mathbf{k}\cdot x_A}, \\
 T^{0i}(t, \mathbf{k})|_{S^1} &= \frac{1}{2} \sum_A S_A^{ij} i\mathbf{k}^j e^{-i\mathbf{k}\cdot x_A}, \\
 T^{ij}(t, \mathbf{k})|_{S^1} &= \frac{1}{2} \sum_A \left( S_A^{il} v_A^j + S_A^{jl} v_A^i \right) i\mathbf{k}^l e^{-i\mathbf{k}\cdot x_A},
 \end{aligned} \tag{62}$$

where a mixed coordinate-momentum space has been adopted, and the leading  $O(S_A^2)$  are given by

$$T^{00}(t, \mathbf{k})|_{S^2} = - \sum_A \frac{C_{ES^2}^{(A)}}{2m_A} S_A^{ik} S_A^{jk} \mathbf{k}_i \mathbf{k}_j e^{-i\mathbf{k}\cdot x_A}, \tag{63}$$

with  $T^{ij}|_{S^2} \sim vT^{0i}|_{S^2} \sim v^2T^{00}$ . Since  $S^{0i}k \sim S^{ij}vk \sim mv^3$  (we recall that  $k \sim 1/r$  is the wave number exchanged between binary constituents), the above components of the energy momentum tensor can be used to compute the source moments necessary to derive physical observables, as discussed in the next subsections. At leading order in spin and  $v$ , the electric and magnetic quadrupole moments read (using the covariant SSC)

$$\begin{aligned}
 I_{ij}|_{S^1} &\supset \sum_A \frac{8}{3} \epsilon^{ikl} \left( v_{Ak} S_l x_{Aj} - \frac{4}{3} x_{Ak} S_l v_{Aj} - \frac{4}{3} x_{Ak} \dot{S}_{Al} x_{Aj} + i \leftrightarrow j \right), \\
 J_{ij}|_{S^1} &\supset \sum_A S_{Ai} x_{Aj} + S_{Aj} x_{Ai},
 \end{aligned} \tag{64}$$

where  $S^i = \epsilon^{ijk} S_{kl}$ . For non-linear terms one has to add diagrams at the orbital scale analogous to figs.15,16 with spin insertion at the vertices, as well as the  $O(S_A^2)$  term in the world-line energy momentum tensor in eq. (62), which translates to quadratic terms in the quadrupole moments given by

$$\begin{aligned}
 I^{ij}|_{S_A^2} &\supset - \sum_A \frac{C_{ES^2}^{(A)}}{m_A} \left( S_A^i S_A^j + S_A^j S_A^i \right), \\
 J_{ij}|_{S_A^2} &\supset \sum_A \frac{C_{ES^2}^{(A)}}{m_A} \left( \epsilon_{ikl} v^k S_A^l S_{Aj} + i \leftrightarrow j \right).
 \end{aligned} \tag{65}$$

### 4.3. Integrating out the radiating graviton: radiation reaction

We have now built an effective theory for extended objects in terms of the source moments and also shown how to match the orbital scale with the theory describing two point particles experiencing mutual gravitational attraction. We can further use the extended object action in eq. (1) to integrate out the gravitational radiation to obtain an effective action  $S_{mult}$  for the source multipoles alone.

In order to perform such computation, boundary conditions *asymmetric in time* have to be imposed, as no incoming radiation at past infinity is required. Using the standard *Feynman* propagator, which ensures a pure in-(out-)going wave at past (future)

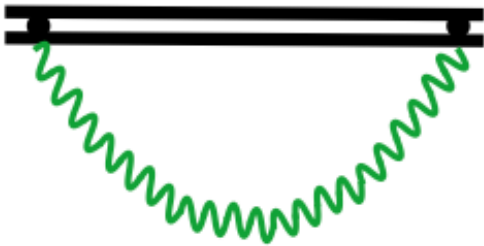


**Figure 17.** Diagram giving the leading term of the amplitude describing radiation back-reaction on the sources.

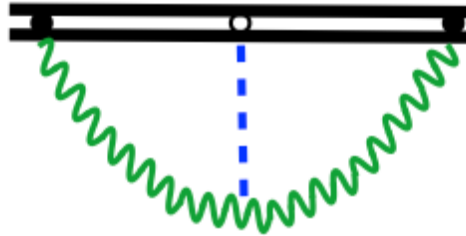


**Figure 18.** Next-to-leading order term in the back-reaction amplitude.

infinity, would lead to a non-causal evolution as it can be shown by looking at the following toy model [72], which is defined by a scalar field  $\Psi$  coupled to a source  $J$ :

$$S_{toy} = \int d^{d+1}x \left[ -\frac{1}{2} (\partial\psi)^2 + \psi J \right]. \quad (66)$$

We may recover the field generated by the source  $J$  as

$$\psi(t, x) = \int d^{d+1}x' G(t - t', x - x') J(t', x'), \quad (67)$$

where the Feynman propagator given by eq. (10) can also be written as

$$G(t, x) = \theta(t) \Delta_+(t, x) + \theta(-t) \Delta_-(t, x), \quad (68)$$

with  $\Delta_{\pm} = e^{\mp i\omega t} e^{i\mathbf{k}\cdot\mathbf{x}}/k$ , which is clearly a-causal because of the  $\theta(-t)$  term. In a causal theory  $\psi$  would be given by the same eq. (67) but with the Feynman propagator replaced by the retarded one  $G_{Ret}(t, x)$ , given by:

$$\begin{aligned} G_{Ret}(t, x) &= - \int_{\mathbf{k}} \frac{d\omega}{2\pi} \frac{e^{-i\omega t + i\mathbf{k}\cdot\mathbf{x}}}{\mathbf{k}^2 - (\omega + i\epsilon)^2} \\ &= -i\theta(t) [\Delta_+(t, x) - \Delta_-(t, x)] = G_{Adv}(-t, -x). \end{aligned} \quad (69)$$

However it is not possible to naively use the retarded propagator in the action (66), as it would still yield non-causal equations of motions [73]. This problem was not present in the conservative dynamics described in sec.3 as the Feynman Green function with symmetric boundary conditions is the appropriate one to describe a conservative system.

However there is a consistent way to define an action for non-conservative system with asymmetric time boundary condition: by adopting a generalization of the Hamilton's variational principle similar to the closed-time-path, or in-in formalism (first proposed in [74], see [75] for a review) as described in [73], which requires a *doubling* of the field variables. For instance the toy model in eq. (66) is modified so that the generating functional for connected correlation functions in the in-in formalism has the path integral representation

$$e^{iS_{eff}[J_1, J_2]} = \int \mathcal{D}\psi_1 \mathcal{D}\psi_2 \exp \left\{ i \int d^{d+1}x \left[ -\frac{1}{2} (\partial\psi_1)^2 + \frac{1}{2} (\partial\psi_2)^2 - J_1 \psi_1 + J_2 \psi_2 \right] \right\}. \quad (70)$$

In this toy example the path integral can be performed exactly, and using the Keldysh representation [76] defined by  $\Psi_- \equiv \Psi_1 - \Psi_2$ ,  $\Psi_+ \equiv (\Psi_1 + \Psi_2)/2$ , one can write

$$\mathcal{S}_{eff}[J_+, J_-] = \frac{i}{2} \int d^{d+1}x d^{d+1}y J_B(x) G^{BC}(x-y) J_C(y), \quad (71)$$

where the  $B, C$  indices take values  $\{+, -\}$  and

$$G^{BC}(t, \mathbf{x}) = \begin{pmatrix} 0 & iG_{Adv}(t, \mathbf{x}) \\ iG_{Ret}(t, \mathbf{x}) & \frac{1}{2}G_H(t, \mathbf{x}) \end{pmatrix}, \quad (72)$$

where  $G^{++} = 0$  and  $G_{Adv, Ret, H}$  are the usual advanced, retarded propagators and Hadamard function respectively, with  $G_H = \Delta_+ + \Delta_-$ . In our case, the lowest order expression of the quadrupole in terms of the binary constituents world-lines  $x_A$ , i.e.

$$Q_{ij}|_{v^0} = \sum_{A=1}^2 m_A \left( x_{Ai} x_{Aj} - \frac{\delta_{ij}}{d} x_{Ak} x_{Ak} \right), \quad (73)$$

is doubled to

$$\begin{aligned} Q_{-ij}|_{v^0} &= \sum_{A=1}^2 m_A (x_{-Ai} x_{+Aj} + x_{+Ai} x_{-Aj}) - \frac{2}{d} \delta_{ij} x_{+Ak} x_{-Ak}, \\ Q_{+ij}|_{v^0} &= \sum_{A=1}^2 m_A x_{+Ai} x_{+Aj} - \frac{1}{d} \delta_{ij} x_{+A}^2 + O(x_-^2). \end{aligned} \quad (74)$$

The world-line equations of motion that properly include radiation reaction effects are given by

$$0 = \frac{\delta S_{eff}[x_{1\pm}, x_{2\pm}]}{\delta x_{A-}} \Bigg|_{\substack{x_{A-}=0 \\ x_{A+}=x_A}}. \quad (75)$$

At lowest order, by integrating out the radiation graviton, i.e. by computing the diagram in fig. 17, one obtains the Burke-Thorne [77] potential term in the effective action  $S_{mult}$

$$S_{mult}|_{fig. 17} = -\frac{G_N}{5} \int dt Q_{-ij}(t) Q_{+ij}^{(5)}(t), \quad (76)$$

where  $A^{(n)}(t) \equiv d^n A(t)/dt^n$ , which has been derived in the EFT framework in [72]. Corrections to the leading effect appears when considering as in the previous subsection higher orders in the multipole expansion: the 1PN correction to the Burke Thorne potential were originally computed in [78, 33] and re-derived with effective field theory methods in [79].

The genuinely non-linear effect, computed originally in [32, 33] and within effective field theory methods in [80], appears at relative 1.5PN order and it is due to the diagram in fig. 18. The result turns out to have a short-distance singularity which introduces a logarithmic contribution to the effective action (by virtue of eq. (75) only terms linear in  $Q_-$  are kept)

$$\begin{aligned} S_{mult}|_{fig. 18} &= -\frac{1}{5} G_N^2 M \int_{-\infty}^{\infty} \frac{d\omega}{2\pi} \omega^6 \left( \frac{1}{\epsilon} - \frac{41}{30} + i\pi - \log \pi + \gamma + \log(\omega^2/\mu^2) \right) \\ &\quad [Q_{ij-}(\omega) Q_{ij+}(-\omega) + Q_{ij-}(-\omega) Q_{ij+}(\omega)]. \end{aligned} \quad (77)$$

We note the presence of the logarithmic term which is non-analytic in  $k$ -space and non-local (but causal) in direct space: after integrating out a mass-less propagating degree of freedom the effective action is not expected to be local [81]. A local mass counter term  $M_{ct}$  defined by

$$M_{ct} = -\frac{2G_N^2}{5}M \left( \frac{1}{\epsilon} + \gamma - \log \pi \right) Q_{-ij} Q_{+ij}^{(6)} \quad (78)$$

can be straightforwardly added to the world-line effective action to get rid of the divergence appearing as  $\epsilon \rightarrow 0$ . According to the standard renormalization procedure, one can define a renormalized mass  $M^{(R)}(t, \mu)$  for the monopole term in the action (1), depending on time (or frequency) and on the arbitrary scale  $\mu$  in such a way that physical quantities (like the energy or the radiation reaction force) will be  $\mu$ -independent<sup>††</sup>.

The derivation of the  $\mu$  dependence of the renormalized mass was first obtained in [82] by evaluating  $Q_{ij}^2$  corrections to the energy momentum tensor of a binary system. Here we give a simplified version of such derivation, following [80], by deriving the logarithmic corrections to the equations of motion from eq. (77)

$$\delta \ddot{x}_{Ai}(t)|_{log} = -\frac{8}{5}x_{aj}(t)G_N^2M \int_{-\infty}^t dt' Q_{ij}^{(7)}(t') \log[(t-t')\mu]. \quad (79)$$

Separating the logarithm argument into a  $t$ -dependent and a  $t$ -independent part, one gets a logarithmic term not-involving time which gives a *conservative* contribution to the force in eq. (79) which shifts logarithmically the mass of the binary system. The logarithmic mass-shift  $\delta M^{(R)}$  can be determined by requiring that its time derivative balance the acceleration shift given by eq. (79) [52]

$$\frac{d(\delta M^{(R)})}{dt} = -\sum_A m_A \delta \ddot{x}_{Ai} \dot{x}_{Ai}. \quad (80)$$

Substituting eq. (79) into eq. (80) and using the leading order quadrupole moment expression in eq. (73) allows to turn the right hand side of eq. (80) into a total time derivative, enabling to identify the logarithmic mass shift as [52]

$$\delta M^{(R)}|_{log} = -\frac{2G_N^2 M}{5} \left( 2Q_{ij}^{(5)} Q_{ij}^{(1)} - 2Q_{ij}^{(4)} Q_{ij}^{(2)} + Q_{ij}^{(3)} Q_{ij}^{(3)} \right) \log(\mu). \quad (81)$$

Eq. (81) can be rewritten as a renormalization group flow equation [82]

$$\mu \frac{d}{d\mu} M^{(R)}(t, \mu) = -\frac{2G_N^2 M}{5} \left( 2Q_{ij}^{(5)} Q_{ij}^{(1)} - 2Q_{ij}^{(4)} Q_{ij}^{(2)} + Q_{ij}^{(3)} Q_{ij}^{(3)} \right). \quad (82)$$

This classical renormalization of the mass monopole term (which can be identified with the Bondi mass of the system, that does not include the energy radiated to infinity) is explained in [82] by considering that the emitted radiation is scattered by the curved space and then absorbed, hence observers at different distance from the source would not agree on the value of the mass.

The ultraviolet nature of the divergence points to the incompleteness of the effective theory in terms of multipole moments: the terms analytic in  $\omega$  in eq. (77) are sensitive

<sup>††</sup>Note that at the order required in the diagram in fig.18,  $M^{(R)}(t, \mu)$  can be safely treated as a constant  $M$  on both its arguments  $t$  and  $\mu$ .

to the short distance physics and their actual value should be obtained by going to the theory at orbital radius.

The tail term radiation reaction force is responsible for a conservative force at 4PN (as the leading radiation reaction acts at 2.5PN and the tail term is a 1.5PN correction to it), so it must be added to the conservative dynamics coming from the calculation of the effective action not involving gravitational radiation, and indeed it is responsible for the logarithmic term in eq. (26).

#### 4.4. Emitted flux

We have now shown how to perform the matching between the theory of extended objects with multipoles and the theory at the orbital scale. Taking the action for extended bodies in eq. (1) as a starting point, the emitted GW-form and the total radiated power can be computed in terms of the source multipoles by evaluating the probability amplitude  $A_h(\mathbf{k})$  to emit a GW of 4-momentum  $(\omega = |\mathbf{k}|, \mathbf{k})$  and helicity  $h$ , using Feynman diagrams with one external radiating gravitational particle. At leading order the amplitude for the emission of a GW with 3-momentum  $\mathbf{k}$ , helicity  $h$  and polarization tensor  $\epsilon_{ij}$ , is given by the diagram in fig. 19 and results in

$$A_h(\mathbf{k}) = \frac{\mathbf{k}^2}{4\Lambda} Q_{ij} \epsilon_{ij}^*(\mathbf{k}, h). \quad (83)$$

The GW-form can be computed using the closed time path formalism

$$\sigma_{ij}(t, x) \supset -2G_N \Lambda_{ij;kl} \int dt' d^d x' G_R(t - t', x - x') \left[ \ddot{I}_{kl} + \frac{4}{3} \epsilon_{lmn} \dot{J}_{mn,k} - \frac{1}{3} \ddot{I}_{klm,m} \right], \quad (84)$$

where we have introduced the TT-projector  $\Lambda_{ij;kl}$  defined as

$$\Lambda_{ij;kl} = P_{ik} P_{jl} - \frac{1}{d-1} P_{ij} P_{kl}, \quad P_{ij} \equiv \delta_{ij} - n_i n_j, \quad (85)$$

being  $n_i$  the unit vector in the direction of observation, and analog formulae hold for the following multipoles. Analogously to what shown in the previous subsection, we have to take into account the GW interaction with the space time curvature produced by the source itself. Including such effect give rise to a *tail* effect, accounted by the diagram in fig. 20, which gives a contribution to the GW amplitude and phase [34, 83]

$$\sigma_{ij} \supset \Lambda_{ij;kl} \frac{2G}{r} \int \frac{d\omega}{2\pi} e^{i\omega(t-r) + iG_N M \omega \left[ \frac{1}{\epsilon} + \log\left(\frac{\omega}{\mu}\right)^2 + \gamma - \frac{11}{6} \right]} (1 + G_N m |\omega| \pi) I_{kl} \quad (86)$$

The infra-red singularity in the phase of the emitted wave is un-physical as it can be absorbed in a re-definition of time in eq. (86). Moreover any experiment, like LIGO and Virgo for instance, can only probe phase *differences* (e.g. the GW phase difference between the instants when the wave enters and exits the experiment sensitive band) and the un-physical dependencies on the regulator  $\epsilon$  and on the subtraction scale  $\mu$  drops out of any observable.

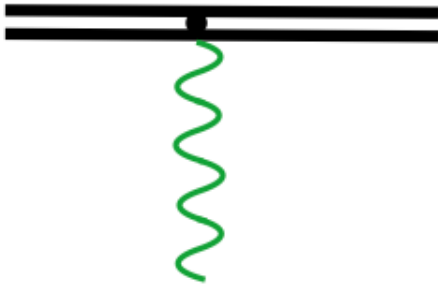


**Figure 19.** Diagram representing the emission of a GW from a quadrupole source

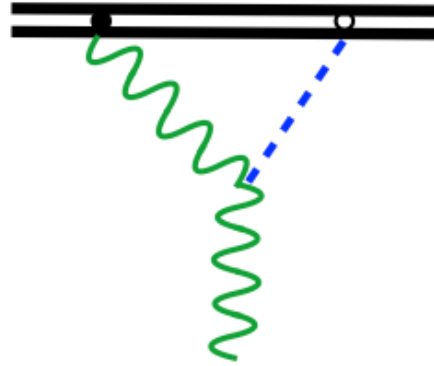


**Figure 20.** Emission of a GW from a quadrupole source with post-Minkowskian correction represented by the scattering off the background curved by the presence of binary system.

The contribution from the magnetic quadrupole is analogous to the one in eq. (86), and it is [83]

$$\sigma_{ij} \supset \Lambda_{ij;kl} \frac{2G}{r} \int \frac{d\omega}{2\pi} e^{i\omega(t-r)+iG_N M\omega \left[ \frac{1}{\epsilon} + \log\left(\frac{\omega}{\mu}\right)^2 + \gamma - \frac{7}{3} \right]} (1 + G_N m |\omega| \pi) J_{kl} \quad (87)$$

where the finite number associated with the logarithm is still un-physical, as it depends on the choice of the arbitrary scale  $\mu$ , but the difference between the terms in the phase in eqs. (86, 87) is physical, as  $\mu$  can be chosen only once [83]. Spin effects can be included straightforwardly by using the appropriate multipole expression.

The total emitted flux can be computed once the amplitude of the GW has been evaluated, via the standard formula

$$P = \frac{r^2}{32\pi G_N} \int d\Omega \langle \dot{h}_{ij} \dot{h}_{ij} \rangle, \quad (88)$$

but there is actually a shortcut, as the emission energy rate can be computed directly from the amplitude  $A_h(\mathbf{k})$  without solving for  $\sigma_{ij}$  via the optical theorem formula

$$dP_h(\omega) = \frac{1}{T} \frac{d^3\mathbf{k}}{(2\pi)^3} |A_h(\mathbf{k})|^2. \quad (89)$$

Using eqs. (83), (89) and summing over polarizations one gets [69]

$$P \simeq \frac{G_N}{5\pi T} \int_0^\infty d\omega \omega^6 \left[ |I_{ij}(\omega)|^2 + \frac{16}{9} |J_{ij}(\omega)|^2 + \frac{5}{189} k^2 |I_{ijk}(\omega)|^2 + \dots \right] \quad (90)$$

which, once averaged over time, recovers at the lowest order the standard Einstein quadrupole formula  $P = G_N \langle \ddot{I}_{ij}^2 \rangle / 5$ . There are however corrections to this result for any given multipole, due to the scattering of the GW off the curved space-time because of the presence of the static potential due to the presence of the massive binary system.

The first of such corrections scale as  $G_N M \int (d^4 k \frac{1}{k})^2 \delta^3(k) \sim G_N M k \sim v^3$  (for radiation  $k \sim v/r$ ), that is a 1.5PN correction with respect to the leading order. The tail amplitude is described by the diagram in fig. 20 and it adds up to the leading order to give a contribution to the flux going as

$$\left| \frac{A_h|_{v^3}}{A_h|_{v^0}} \right|^2 = 1 + 2\pi G_N M \omega + O(v^6). \quad (91)$$

The diagrams quadratic in the background curvature are portrayed in figs. 21 and they give an ultraviolet divergence, with a logarithmic term [69]

$$\left| \frac{A_h|_{v^6}}{A_h|_{v^0}} \right|_{v^6}^2 = -(G_N M \omega)^2 \frac{214}{105} \ln \frac{\omega^2}{\mu^2} + \dots, \quad (92)$$

depending on the arbitrary subtraction scale  $\mu$ , where finite contributions have been omitted. This short-distance singularity represents a failure of the effective theory at the radiation scale to correctly describe short-distance physics: in order to fix the omitted numerical quantity analytic in  $\omega$  one should match the multipole theory to the theory in which the binary constituents are at a finite distance  $r$ .

However the coefficient of the logarithm is physical and we can then proceed to renormalize the theory at the radiation scale, which is done in the usual fashion as in quantum field theory, although here the effect is completely classical. Since  $|A_h|^2$  enters physical results like energy emission, it should be independent of the arbitrary scale  $\mu$ : this can only happen if we assume a  $\mu$  dependence on the *renormalized* multipole moments  $I_{ij}$  of the type:

$$\mu \frac{dI_{ij}^{(R)}}{d\mu} = -\frac{214}{105} (G_N M \omega)^2 I_{ij}^{(R)}. \quad (93)$$

Assuming that  $A_h$  is expressed in terms of the  $I_{ij}^{(R)}$ , the total dependence of  $|A_h|^2$  on  $\mu$  cancels out (it makes no difference if using  $I_{ij}^{(R)}$  or the “bare”  $I_{ij}$  in  $A_h|_{v^3}$ , as the difference is higher order in  $v$ ). The background curvature has the effect of “smearing” the multipole source which cannot be considered perfectly localized at the origin of the coordinates: the value of the  $I_{ij}^{(R)}$  will depend on the scale at which the observer will measure it.

A consequence of this result is that eq. (93) admits a solution

$$I_{ij}^{(R)}(k, \mu) = \left( \frac{\mu}{\mu_0} \right)^{-\frac{214}{105} (G_N M \omega)^2} I_{ij}(k, \mu_0) \quad (94)$$

that constrains the patterns of logarithms that can appear at higher orders. Once the multipole is known at some scale, like the orbital scale separation, then it can be known at any other scale by virtue of eq. (94).

Finally one could consider the scattering of the emitted GW wave off another GW, as in fig. 22. This process is known as *non-linear memory* effect, it represents a 2.5PN correction with respect to the leading emission amplitude [84, 85, 86] and it has not yet been computed within the effective field theory formalism.

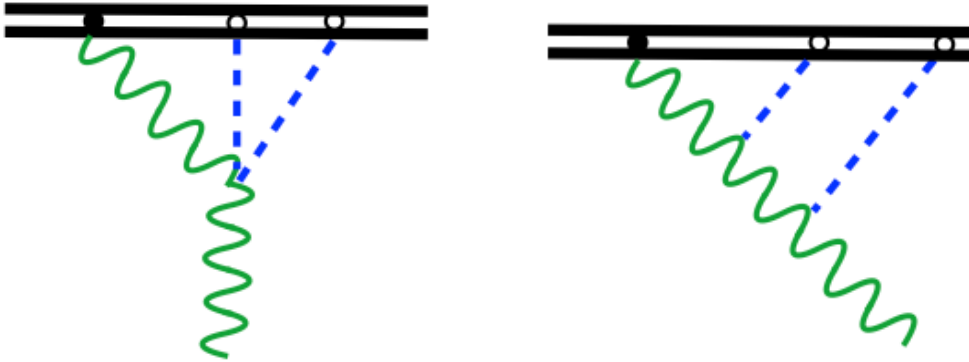


**Figure 21.** Diagrams contributing to  $A_h(k)|_{v^6}$ .

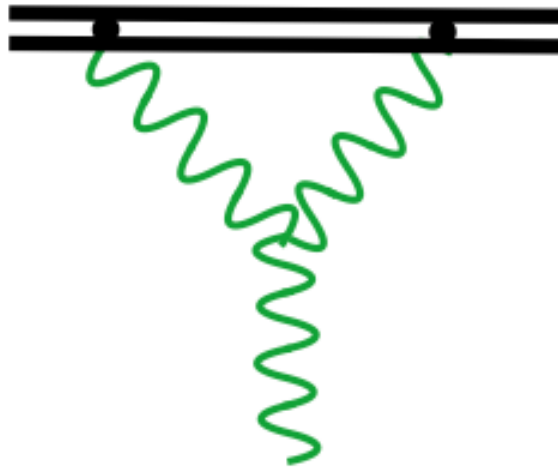


**Figure 22.** Memory diagram: GW emitted from a source scattered by another GW before reaching the observer.

Combined tail and memory effects enter at 4PN order in the emitted radiation, i.e. double scattering of the emitted radiation off the background curvature *and* off another GW. The divergences describing such process have been analyzed in [82], leading to the original derivation of the mass renormalization described in subsec. 4.3. The renormalization group equations allow a resummation of the logarithmic term making a non-trivial prediction for the pattern of the leading UV logarithms appearing at higher orders [69, 82].

## 5. Conclusions

This Topical Review aims at giving an overview of the basic ideas of Effective Field Theory methods proposed in [12] to model gravitationally bound, inspiralling compact binary systems. The study of such system has both phenomenological and theoretical



motivations, due to the forthcoming observational campaign of the large interferometric detectors LIGO and Virgo (and eventually KAGRA and Indigo) on one side, and on the development of efficient numerical methods to solve Einstein equations on the other side.

The post-Newtonian investigation of the compact binary inspiral problem has a long history in analytical perturbative solutions of the Einstein equations, but EFT methods have allowed a new field theory insight into it. The problem admits a description in terms of well separated scales (the individual source size, the binary component distance and the radiation wavelength), with a single dimension-less perturbative parameter (at least in the binary black-hole case), represented by the relative velocity of the individual components of the binary system. The EFT methods allow to treat in a single, powerful framework both conservative and dissipative effects and provide efficient tools to compute observable quantities. They give an organizational principle for performing a systematic expansion in the PN perturbative parameter. The scale factorization is already evident at the level of the action, which allows a considerable computational simplification with respect to methods working at the level of the equations of motion. The effective field theory approach reviewed here has much in common with standard quantum field theory techniques because of the common underlying field theory structure and it is completely classic.

Physics at different scales are related by renormalization group flow, and all kind of divergences, arising from incomplete knowledge of the underlying short-distance physics as well as from long-distance effects and from gauge artifacts, are technically treated on equal footing via dimensional regularization. Indeed the use of field theory since several decades has allowed the development of powerful tools to address all the technical problems (like handling of divergences and computation of Feynman integrals) on the computational side.

Finally, the existence of an additional independent method to compute physical observables of the binary problem in General Relativity is welcome *per se*, as it allows an independent check of computations of formidable complexity.

## Acknowledgments

SF is supported by the Fonds National Suisse, RS is supported by the FAPESP grant 2013/04538-5. RS wishes to thank the CERN theory division for hospitality and support during the last stage of this work.

## References

- [1] R A Hulse and J H Taylor. Discovery of a pulsar in a binary system. *Astrophys. J.*, 195:L51, 1975.
- [2] J. M. Weisberg and J. H. Taylor. Observations of post-newtonian timing effects in the binary pulsar psr 1913+16. *Phys. Rev. Lett.*, 52:1348, 1984.

- [3] M. Burgay, N. D'Amico, A. Possenti, R. N. Manchester, A. G. Lyne, B. C. Joshi, M. A. McLaughlin, and M. Kramer *et al.* An increased estimate of the merger rate of double neutron stars from observations of a highly relativistic system. *Nature*, 426:531, 2003.
- [4] M. Kramer and N. Wex. The double pulsar system: A unique laboratory for gravity. *Class. Quant. Grav.*, 26:073001, 2009.
- [5] A. Wolszczan. A nearby 37.9-ms radio pulsar in a relativistic binary system. *Nature*, 350:688, 1991.
- [6] I. H. Stairs, S. E. Thorsett, J. H. Taylor, and A. Wolszczan. Studies of the relativistic binary pulsar psr b1534+12: I. timing analysis. *Astrophys. J.*, 581:501, 2002.
- [7] J. Aasi *et al.* Search for Gravitational Waves from Binary Black Hole Inspiral, Merger and Ringdown in LIGO-Virgo Data from 2009-2010. *Phys.Rev.*, D87:022002, 2013.
- [8] *LIGO/Virgo/GEO/KAGRA Science*, volume 467 of *ASP Conference Series*. Astronomical Society of the Pacific, 2012.
- [9] Yoichi Aso, Yuta Michimura, Kentaro Somiya, Masaki Ando, Osamu Miyakawa, *et al.* Interferometer design of the KAGRA gravitational wave detector. 2013.
- [10] LIGO Scientific and Virgo Collaborations. Predictions for the rates of compact binary coalescences observable by ground-based gravitational-wave detectors. *Class. Quant. Grav.*, 27:173001, 2010.
- [11] Luc Blanchet. Gravitational radiation from post-newtonian sources and inspiralling compact binaries. *Living Reviews in Relativity*, 9(4), 2006.
- [12] Walter D. Goldberger and Ira Z. Rothstein. An Effective field theory of gravity for extended objects. *Phys.Rev.*, D73:104029, 2006.
- [13] W. D. Goldberger. Les houches lectures on effective field theories and gravitational radiation. In *Les Houches Summer School - Session 86: Particle Physics and Cosmology: The Fabric of Spacetime*, 2007.
- [14] Bruno Bertotti and Jerzy Plebanski. Theory of gravitational perturbations in the fast motion approximation. *Ann.Phys.*, 11:169, 1960.
- [15] N.D. Hari Dass and V. Soni. FEYNMAN GRAPH DERIVATION OF EINSTEIN QUADRUPOLE FORMULA. *J.Phys.*, A15:473, 1982.
- [16] Thibault Damour and Gilles Esposito-Farese. Testing gravity to second postNewtonian order: A Field theory approach. *Phys.Rev.*, D53:5541–5578, 1996.
- [17] P.C. Peters and J. Mathews. Gravitational radiation from point masses in a Keplerian orbit. *Phys.Rev.*, 131:435–439, 1963.
- [18] M. Maggiore. *Gravitational Waves*. Oxford University Press, 2008.
- [19] Ian Hinder and Alessandra *et al.* Buonanno. Error-analysis and comparison to analytical models of numerical waveforms produced by the nrar collaboration. arXiv:1307.5307.
- [20] M. Hannam F. Ohme and S. Husa. Reliability of complete gravitational waveform models for compact binary coalescences. *Phys. Rev.*, D84:064029, 2011.
- [21] H. Georgi. An effective field theory for heavy quarks at low-energies. *Phys. Lett. B*, 240:447, 1990.
- [22] N. Isgur and M. B. Wise. Spectroscopy with heavy quark symmetry. *Phys. Rev. Lett.*, 66:1130, 1991.
- [23] Walter D. Goldberger and Ira Z. Rothstein. Dissipative effects in the worldline approach to black hole dynamics. *Phys.Rev.*, D73:104030, 2006.
- [24] T. Damour. *Gravitational radiation and the motion of compact bodies*, pages 59–144. North-Holland, Amsterdam, 1983.
- [25] T. Damour. Gravitational radiation and the motion of compact bodies. In N. Deruelle and T. Piran, editors, *Gravitational Radiation*, pages 59–144. North-Holland, Amsterdam, 1983.
- [26] Barak Kol and Michael Smolkin. Black hole stereotyping: Induced gravito-static polarization. *JHEP*, 1202:010, 2012.
- [27] Barak Kol and Michael Smolkin. Non-Relativistic Gravitation: From Newton to Einstein and Back. *Class.Quant.Grav.*, 25:145011, 2008.
- [28] Barak Kol and Michael Smolkin. Classical Effective Field Theory and Caged Black Holes.

- Phys.Rev.*, D77:064033, 2008.
- [29] L. Blanchet and T. Damour. POSTNEWTONIAN GENERATION OF GRAVITATIONAL WAVES. *Annales Poincare Phys.Theor.*, 50:377–408, 1989.
- [30] J. F. Donoghue. General relativity as an effective field theory: The leading quantum corrections. *Phys. Rev. D*, page 3874, 1994.
- [31] I. Z. Rothstein. Tasi lectures on effective field theories. TASI lecture.
- [32] Luc Blanchet and Thibault Damour. Tail transposed temporal correlations in the dynamics of a gravitating system. *Phys.Rev.*, D37:1410, 1988.
- [33] L. Blanchet. Time asymmetric structure of gravitational radiation. *Phys.Rev.*, D47:4392–4420, 1993.
- [34] L. Blanchet and Gerhard Schafer. Gravitational wave tails and binary star systems. *Class.Quant.Grav.*, 10:2699–2721, 1993.
- [35] Barak Kol and Michael Smolkin. Einstein’s action and the harmonic gauge in terms of Newtonian fields. *Phys.Rev.*, D85:044029, 2012.
- [36] James B. Gilmore and Andreas Ross. Effective field theory calculation of second post-Newtonian binary dynamics. *Phys.Rev.*, D78:124021, 2008.
- [37] Yi-Zen Chu. The n-body problem in General Relativity up to the second post-Newtonian order from perturbative field theory. *Phys.Rev.*, D79:044031, 2009.
- [38] Stefano Foffa and Riccardo Sturani. Effective field theory calculation of conservative binary dynamics at third post-Newtonian order. *Phys.Rev.*, D84:044031, 2011.
- [39] Stefano Foffa and Riccardo Sturani. The dynamics of the gravitational two-body problem in the post-Newtonian approximation at quadratic order in the Newton’s constant. *Phys.Rev.*, D87:064011, 2013.
- [40] Piotr Jaranowski and Gerhard Schafer. Towards the 4th post-Newtonian Hamiltonian for two-point-mass systems. *Phys.Rev.*, D86:061503, 2012.
- [41] Piotr Jaranowski and Gerhard Schfer. Dimensional regularization of local singularities in the 4th post-Newtonian two-point-mass Hamiltonian. *Phys. Rev.*, D87:081503, 2013.
- [42] Barak Kol and Ruth Shir. Classical 3-loop 2-body diagrams. 2013.
- [43] A. von Manteuffel and C. Studerus. Reduze 2 - Distributed Feynman Integral Reduction. 2012.
- [44] Stefano Foffa, Pierpaolo Mastrolia, Riccardo Sturani, and Christian Sturm. In preparation.
- [45] Barak Kol and Michael Smolkin. Dressing the Post-Newtonian two-body problem and Classical Effective Field Theory. *Phys.Rev.*, D80:124044, 2009.
- [46] Duff Neill and Ira Z. Rothstein. Classical Space-Times from the S Matrix. 2013.
- [47] Thibault Damour, Piotr Jaranowski, and Gerhard Schafer. Dimensional regularization of the gravitational interaction of point masses. *Phys.Lett.*, B513:147–155, 2001.
- [48] Yousuke Itoh. Equation of motion for relativistic compact binaries with the strong field point particle limit: Third postNewtonian order. *Phys.Rev.*, D69:064018, 2004.
- [49] Luc Blanchet and Guillaume Faye. Equations of motion of point particle binaries at the third postNewtonian order. *Phys.Lett.*, A271:58, 2000.
- [50] Luc Blanchet and Guillaume Faye. General relativistic dynamics of compact binaries at the third postNewtonian order. *Phys.Rev.*, D63:062005, 2001.
- [51] Vanessa C. de Andrade, Luc Blanchet, and Guillaume Faye. Third postNewtonian dynamics of compact binaries: Noetherian conserved quantities and equivalence between the harmonic coordinate and ADM Hamiltonian formalisms. *Class.Quant.Grav.*, 18:753–778, 2001.
- [52] A. Le Tiec L. Blanchet, S. L. Detweiler and B. F. Whiting. High-order post-newtonian fit of the gravitational self-force for circular orbits in the schwarzschild geometry. *Phys. Rev.*, D81, 2010.
- [53] Alexandre Le Tiec, Luc Blanchet, and Bernard F. Whiting. The First Law of Binary Black Hole Mechanics in General Relativity and Post-Newtonian Theory. *Phys.Rev.*, D85:064039, 2012.
- [54] Donato Bini and Thibault Damour. Analytical determination of the two-body gravitational interaction potential at the 4th post-Newtonian approximation. 2013.
- [55] Rafael A. Porto and Ira Z. Rothstein. The Hyperfine Einstein-Infeld-Hoffmann potential.

- Phys.Rev.Lett.*, 97:021101, 2006.
- [56] Rafael A. Porto. New results at 3PN via an effective field theory of gravity. *Proceedings of the MG11 Meeting on General Relativity*, pages 2493–2496, 2007.
- [57] Rafael A Porto and Ira Z. Rothstein. Next to Leading Order Spin(1)Spin(1) Effects in the Motion of Inspiralling Compact Binaries. *Phys.Rev.*, D78:044013, 2008.
- [58] Johannes Hartung and Jan Steinhoff. Next-to-next-to-leading order post-Newtonian spin(1)-spin(2) Hamiltonian for self-gravitating binaries. *Annalen Phys.*, 523:919–924, 2011.
- [59] Michele Levi. Binary dynamics from spin1-spin2 coupling at fourth post-Newtonian order. *Phys.Rev.*, D85:064043, 2012.
- [60] Sylvain Marsat, Alejandro Bohé, Guillaume Faye, and Luc Blanchet. Next-to-next-to-leading order spin-orbit effects in the equations of motion of compact binary systems. *Class.Quantum Grav.*, 30:055007, 2013.
- [61] Alejandro Bohé, Sylvain Marsat, Guillaume Faye, and Luc Blanchet. Next-to-next-to-leading order spin-orbit effects in the near-zone metric and precession equations of compact binaries. *Class.Quant.Grav.*, 30:075017, 2013.
- [62] Alejandro Bohé, Sylvain Marsat, and Luc Blanchet. Next-to-next-to-leading order spin-orbit effects in the gravitational wave flux and orbital phasing of compact binaries. *Class.Quant.Grav.*, 30:135009, 2013.
- [63] Rafael A. Porto. Post-Newtonian corrections to the motion of spinning bodies in NRGR. *Phys.Rev.*, D73:104031, 2006.
- [64] Rafael A. Porto and Ira Z. Rothstein. Spin(1)Spin(2) Effects in the Motion of Inspiralling Compact Binaries at Third Order in the Post-Newtonian Expansion. *Phys.Rev.*, D78:044012, 2008.
- [65] Rafael A. Porto. Next to leading order spin-orbit effects in the motion of inspiralling compact binaries. *Class.Quant.Grav.*, 27:205001, 2010.
- [66] Thibault Damour, Piotr Jaranowski, and Gerhard Schaefer. Hamiltonian of two spinning compact bodies with next-to-leading order gravitational spin-orbit coupling. *Phys.Rev.*, D77:064032, 2008.
- [67] Enrico Barausse, Etienne Racine, and Alessandra Buonanno. Hamiltonian of a spinning test-particle in curved spacetime. *Phys.Rev.*, D80:104025, 2009.
- [68] Steven Hergt, Jan Steinhoff, and Gerhard Schaefer. On the comparison of results regarding the post-newtonian approximate treatment of the dynamics of extended spinning compact binaries. 2012.
- [69] W. D. Goldberger and A. Ross. Gravitational radiative corrections from effective field theory. *Phys. Rev. D*, 81:124015, 2010.
- [70] Andreas Ross. Multipole expansion at the level of the action. *Phys.Rev.*, D85:125033, 2012.
- [71] A. Ross R. A. Porto and I. Z. Rothstein. Spin induced multipole moments for the gravitational wave flux from binary inspirals to third post-newtonian order. *JCAP*, 2011.
- [72] M. Tiglio C. R. Galley. Radiation reaction and gravitational waves in the effective field theory approach. *Phys. Rev.*, D79:124027, 2009.
- [73] C. R. Galley. The classical mechanics of non-conservative systems. *Phys. Rev. Lett.*, 110:174301, 2013.
- [74] J. S. Schwinger. Brownian motion of a quantum oscillator. *J. Math. Phys.*, 2:407–432, 1961.
- [75] B. DeWitt. Effectice action for expectation values. In R. Penrose and C. J. Isham, editors, *Quantum concepts in Space and Time*. Clarendon Press, Oxford, 1986.
- [76] L. V. Keldysh. Diagram technique for nonequilibrium processes. *Zh. Eksp. Teor. Fiz.*, 47:1515–1527, 1964.
- [77] W. L. Burke and K. S. Thorne. Gravitational radiation damping. In S. I. Fickler M. Carmeli and L. Witten, editors, *Relativity*, pages 209–228. Plenum, New York, 1970.
- [78] B. R. Iyer and C. M. Will. Postnewtonian gravitational radiation reaction for two-body systems. *Phys. Rev. Lett.*, 70:113, 1993.
- [79] C. R. Galley and A. K. Leibovich. Radiation reaction at 3.5 post-newtonian order in effective field

- theory. *Phys. Rev. D*, 86:044029, 2012.
- [80] S. Foffa and R. Sturani. Tail terms in gravitational radiation reaction via effective field theory. *Phys. Rev. D*, 87:044056, 2013.
- [81] T. Appelquist and J. Carazzone. Infrared singularities and massive fields. *Phys. Rev. D*, 11:2856, 1975.
- [82] A. Ross W. D. Goldberger and I. Z. Rothstein. Black hole mass dynamics and renormalization group evolution. arXiv:1211.6095 [hep-th].
- [83] A. Ross R. A. Porto and I. Z. Rothstein. Spin induced multipole moments for the gravitational wave amplitude from binary inspirals to 2.5 post-newtonian order. *JCAP*, 1209:028, 2012.
- [84] D. Christodoulou. Nonlinear nature of gravitation and gravitational wave experiments. *Phys.Rev.Lett.*, 67:1486–1489, 1991.
- [85] Luc Blanchet and Thibault Damour. Hereditary effects in gravitational radiation. *Phys.Rev.*, D46:4304–4319, 1992.
- [86] Luc Blanchet. Gravitational wave tails of tails. *Class.Quant.Grav.*, 15:113–141, 1998.